The moving and settling of plastic in the ocean

Forward and reverse time modelling of plastic particles

E. J. Burgers

The moving and settling of plastic in the ocean

Forward and reverse time modelling of plastic particles

by

E. J. Burgers

Part of the Bachelors Applied Mathematics and Applied Physics
at the Delft University of Technology.

Student number:	4395476	
Project duration:	September 1, 2017 – August 22, 2018	
Committee:	Prof. dr. ir. A. W. Heemink	TU Delft (Supervisor)
	Dr. ir. M. Rohde	TU Delft (Supervisor)
	Dr. D. J. P. Lahaye	TU Delft
	Dr. Z. Perko	TU Delft

An electronic version of this thesis is available at `http://repository.tudelft.nl/`.

Cover image: *Pollution dans un port Maltais* by Alain Bachellier

TU Delft

Abstract

The growing amount of plastic pollution in the oceans is worldwide a huge problem. There is an increasing amount of projects that try to clean up this pollution. To remove the pollution efficiently, it is useful to know how plastic litter moves, degrades and sinks. Models are being developed that can describe what happens with plastic in the ocean.

To model the behaviour of plastic in the ocean a lot of parameters need to be taken into account. The transport of plastic particles is largely determined by processes like the wind and the current but their movement also has a random character due to dispersion. Due to this random movement, the future position of a particle can be described by a probability distribution. To find that probability distribution, the Kolmogorov forward equation (or Fokker-Planck equation), in this context the same as the advection-diffusion equation, needs to be solved.

It is also possible that the plastic particles sink and settle on the bottom of the ocean. One goal of this project was to incorporate the settling of particles as an extra term into the advection-diffusion equation.

Forward models are used to predict where particles will go to. It can also be useful to have reverse time models that can describe where particles had their origin. To make reverse time models, it is necessary to solve a reverse time advection-diffusion equation. The main goal of this project was to derive and solve the reverse time advection-diffusion equation that includes the settling of particles. This is done by finding the adjoint of the Kolmogorov forward equation and the settling term.

Contents

1 Introduction

Plastic pollution is worldwide a huge problem. The use of plastic has quickly increased in the last decades and is expected to increase even more in the future. Consequently there is also an increasing amount of plastic that ends up in our oceans. For example in 2010, 192 coastal countries produced a total of 275 million tons of plastic waste and between 4.8 and 12.7 million tons of plastic entered the oceans (Jambeck et al. [10]).

This does a lot of harm to the ecosystems in the oceans. Animals can get entangled or think the plastic is food, eat it and possibly die due to smothering or famine. The plastic could also end up in the food chain and consequently do harm to other animals as well. Eventually this could even threaten human health. For these reasons there is an increasing number of projects that aim to reduce the amount of plastic waste in our oceans. This can either be done by making sure there is less waste entering the ocean or by cleaning up the waste that is already there. To optimise the effectiveness of plastic waste removal it is necessary to know how the plastic litter moves, degrades and sinks.

1.1. Introduction to plastic models

Models are being developed that can describe what happens with plastic particles in the ocean. Unfortunately this is quite complex to model. There is a large amount of processes and parameters that need to be taken into account to make an accurate model. The most important processes and parameters will be introduced here.

Of course the direction and magnitude of the current have a large effect on the movement of plastic particles. When a particle is floating, the wind can also have an important influence on the transportation. The magnitude of the wind effect is determined by the wind drift coefficient. The value of this coefficient depends on the shape, size and buoyancy of the plastic. Naturally the wind has a greater influence on larger, more buoyant and less aerodynamic objects.

Not only the wind and the current are affecting the movement of plastic particles. Dispersion also needs to be taken into account. This is the movement of particles due to small irregularities in the velocity field. It is the random movement particles in the water appear to have and causes particles to spread when they are released in the same position. The magnitude of this random movement depends on the turbulence of the water but can also be defined larger if the knowledge of the velocity field is not very precise.

Different plastic objects vary in properties like shape, size, density etc., this does not only affect the wind drift coefficient but also the speed of degradation. Plastic degrades while it is in the water and the speed of this process depends on the type of plastic and the marine environment. Due to degradation, but also absorbing water or other substances and biofouling (a layer of micro-organisms accumulating on the surface) plastic particles can also sink and settle on the bottom of the ocean. So the type of plastic and marine environment also influence the settling rate of plastic particles.

Clearly a lot of parameters have to be taken into account to make an accurate model. Therefore these models are made for specific geographical areas and moments in time. This report focusses on the mathematical and physical background of these models instead of finding the best parameters for a specific situation. The gained knowledge can be used to make an improved general model that can simulate a specific time and area by implementing the suitable parameters. The model of this project is mainly based on Critchell and Lambrechts [4] and that model is visualised in figure 1.1.

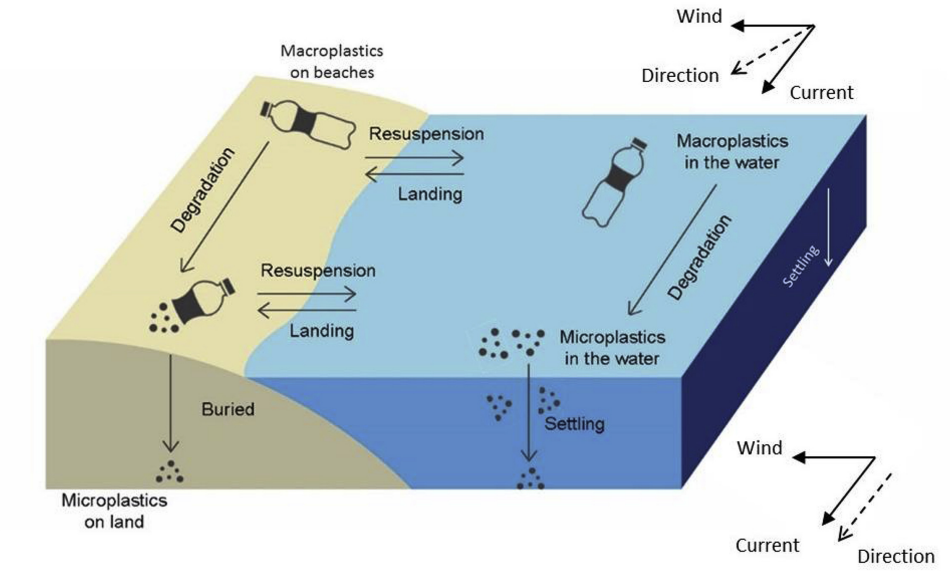

Figure 1.1: This image shows the possibilities of what can happen to plastic particles when they are located in coastal waters (Critchell and Lambrechts [4]).

This model starts with macroplastics that entered the coastal water. Macroplastics are defined as plastic with a size larger than 5 mm, which means that macroplastics could be almost all the plastic trash imaginable (bottles, bags, packaging, etc.). In general the macroplastics will float on the water. Over time a few things can happen with a macroplastic. The macroplastic will move due to processes like wind and current but also dispersion has an effect on the transportation. The macroplastics could land on the beach and there either be buried or resuspended in the ocean. Apart from moving, the macroplastics could also sink and settle on the bottom of the ocean. Once settled, it is assumed the particles stop moving. Last but not least, the macroplastics can degrade, creating microplastics, which are plastic particles with a size smaller than 5 mm.

Unlike macroplastics, microplastics are assumed to be spread through the water column instead of floating on the water. This means that when they move, they will not be affected by the wind. Just like macroplastics, they also have a chance to settle to the bottom of the ocean. Microplastics can also land on the beach and there again either be buried or resuspended.

In this report the landing on the beach of both macro- and microplastics is not taken into account.

1.2. Goals of this project

There are already models that describe the movement of both macro- and microplastics in the oceans. As said, the movement of plastic particles is not only depending on physical conditions like the wind and current but also has a random character due to dispersion. Dispersion can be regarded as molecular diffusion but on a larger scale. The advection-diffusion equation can be used in situations with both advective and diffusive transport. Therefore solving the advection-diffusion equation with the correct parameters can give a solution for the movement of plastic particles in the ocean.

As mentioned above, it is possible that the particles sink and settle on the bottom of the ocean. The standard transport models do not include this settling in the advection-diffusion equation. One goal of this project was to add the settling of plastic particles to the advection-diffusion equation.

There are already a few researches that have added settling of a substance as decay to the advection-diffusion equation. In Charles [2] and van den Boogaard et al. [17], the settling of sediment is added to the

advection-diffusion equation. They are both using a different method to obtain an advection-diffusion equation with a sink term. These two methods are both tried to add the settling of plastic particles to the advection-diffusion equation.

Up until now, only forward time models are mentioned but it can also be useful to have reverse time models. Instead of describing where a particle will go in the future, reverse time models can explain where a particle came from. This can be useful to find the source of pollution. There is not much research done in this area of interest yet but for example in Syed [16] the reverse time advection-diffusion equation is derived and Spivakovs'ka [15] is a research about models with reverse time diffusion.

A reverse time model that includes the settling of particles is not derived yet. Therefore the main goal of this project was to derive and solve the reverse time advection-diffusion equation that includes the settling of particles. To obtain this equation, the forward advection-diffusion equation that includes the settling is used.

1.3. Outline of this report

This report is structured as follows:

In *Chapter 2* some theory on transport models is covered. The derivation of the advection-diffusion equation is shown and the different approaches in solving this equation are introduced.

Chapter 3 begins with some necessary theory of Stochastic Differential Equations. Next, this knowledge will be used to derive the Kolmogorov forward equation (or Fokker-Planck equation). The Kolmogorov backward equation is also obtained in this chapter by finding the adjoint of the forward equation.

In *Chapter 4* the connection between the advection-diffusion equation and the Kolmogorov equations is shown. This leads to a method to numerically approximate the solution of the advection-diffusion equation for both forward and reverse time. Last some information on the drift and diffusion terms of these equations will be provided.

In *Chapter 5* two different methods are used to derive the advection-diffusion equation that includes the settling. The reverse time advection-diffusion equation with settling is also found, again by determining the adjoint of the forward equation. More information on the values for the settling probabilities and rates is also given at the end of this chapter.

Chapter 6 starts with an explanation of the test case used to simulate both the forward and reverse time model. Some simple simulations were done to check if the chosen number of particles and time step are sufficient. Finally the results of the actual simulations will be shown through different figures.

Chapter 7 contains the most important conclusions of this project as well as some suggestions for further research.

2

Transport models

Transport models can be used to describe the movement of pollutants in the ocean. These models are often based on the advection-diffusion equation. This chapter will show the derivation of the advection-diffusion equation for describing the movement of plastic particles. The different approaches in solving this equation will also be introduced.

2.1. Advective and dispersive transport

When a plastic particle enters the ocean, it will move as a result of several physical processes. These processes can be described with partial differential equations. By finding the (numerical) solution of these equations, the movement of plastic particles can be modelled.

The most obvious cause of movement is the waterflow. To describe this movement an advection equation can be used. Advection describes the movement of a quantity due to bulk movements like current or wind. The advection equation is a first order partial differential equation. For a conserved quantity (for example the concentration c), it is the continuity equation:

$$\frac{\partial c}{\partial t} + \nabla(\mathbf{u}c) = 0 \tag{2.1}$$

Here $\mathbf{u}$ is a velocity field.

Particles do not only move due to advective transport but also due to dispersion. Dispersion is the spreading as a result of small local irregularities in the velocity field. Dispersion can be described as molecular diffusion but on a larger scale. Diffusion is spreading due to interactions at a molecular level. The change in concentration due to diffusion can be described by Fick's second law:

$$\frac{\partial c}{\partial t} = D \nabla^2 c \tag{2.2}$$

c is again the concentration and D is the diffusion coefficient. Fick's law is a second order partial differential equation and it describes the spreading of mass in a fluid with no mean velocity.

2.2. Advection-diffusion equation

When a plastic particle is located in the ocean, it will experience a flow with a mean velocity but also spreading due to dispersion. This means that the two partial differential equations of the previous section can be combined to:

$$\frac{\partial c}{\partial t} = -\nabla(\mathbf{u}c) + D \nabla^2 c \tag{2.3}$$

For three dimensions this can also be written as:

$$\frac{\partial c}{\partial t} = -\frac{\partial u_1 c}{\partial x_1} - \frac{\partial u_2 c}{\partial x_2} - \frac{\partial u_3 c}{\partial x_3} + D\left(\frac{\partial^2 c}{\partial x_1^2} + \frac{\partial^2 c}{\partial x_2^2} + \frac{\partial^2 c}{\partial x_3^2}\right) \tag{2.4}$$

This is the base of the advection-diffusion equation, next turbulence will be included in this equation and it will be transformed into a depth-averaged advection-diffusion equation (Spivakovs'ka [15]).

2.2.1. Turbulence

The previous equation describes advection and diffusion in laminar flow but most flows in nature are turbulent. Turbulence consists of 'eddies'(disturbances) of different order. The Reynolds number can be used to decide if a flow is turbulent, this number is defined as:

$$Re = \frac{\rho u L}{\mu} \tag{2.5}$$

Here ρ is the fluid density, u the fluid velocity, L the characteristic length and μ the dynamic viscosity. If Re is low, the flow is laminar and if Re is high, the flow is turbulent. If the value of Re is between the critical values for a high and low Reynolds number, there will be a transition flow. Different geometries have different values for the critical Reynolds number for laminar and turbulent flow.

From now stationary homogeneous turbulence is assumed, so the degree of turbulence remains steady. This means that the variance of the velocity does not change with time or position. The flow and concentration at any point can be written as the time averaged value at that point (respectively $\mathbf{u}$ and c) plus the variation from the average due to turbulence: ($\mathbf{u}'$ and c').

$$\mathbf{U} = \mathbf{u} + \mathbf{u}'$$
$$C = c + c'$$

Substituting this into equation 2.4, gives the following:

$$\frac{\partial C}{\partial t} = -\frac{\partial (u_1 + u_1')(c + c')}{\partial x_1} - \frac{\partial (u_2 + u_2')(c + c')}{\partial x_2} - \frac{\partial (u_3 + u_3')(c + c')}{\partial x_3} + D\left(\frac{\partial^2 c + c'}{\partial x_1^2} + \frac{\partial^2 c + c'}{\partial x_2^2} + \frac{\partial^2 c + c'}{\partial x_3^2}\right) \tag{2.6}$$

This is integrated to obtain the time average, that results in this equation:

$$\frac{\partial c}{\partial t} = -\frac{\partial u_1 c}{\partial x_1} - \frac{\partial u_2 c}{\partial x_2} - \frac{\partial u_3 c}{\partial x_3} - \frac{\partial \overline{u_1' c'}}{\partial x_1} - \frac{\partial \overline{u_2' c'}}{\partial x_2} - \frac{\partial \overline{u_3' c'}}{\partial x_3} + D\left(\frac{\partial^2 c}{\partial x_1^2} + \frac{\partial^2 c}{\partial x_2^2} + \frac{\partial^2 c}{\partial x_3^2}\right) \tag{2.7}$$

Here $\overline{u_i' c'}$ is the time averaged turbulent advective transport. This term can be treated as turbulent diffusion term, which can be incorporated in the diffusion term:

$$D\frac{\partial c}{\partial x_i} - \overline{u_i' c'} = k_i \frac{\partial c}{\partial x_i} \tag{2.8}$$

Filling this in, gives:

$$\frac{\partial c}{\partial t} = -\frac{\partial u_1 c}{\partial x_1} - \frac{\partial u_2 c}{\partial x_2} - \frac{\partial u_3 c}{\partial x_3} + \frac{\partial}{\partial x_1}\left(k_1 \frac{\partial c}{\partial x_1}\right) + \frac{\partial}{\partial x_2}\left(k_2 \frac{\partial c}{\partial x_2}\right) + \frac{\partial}{\partial x_3}\left(k_3 \frac{\partial c}{\partial x_3}\right) \tag{2.9}$$

2.2.2. Depth-averaged

Microplastics are assumed to be spread evenly through the water column. Therefore the concentration of microplastics could also be described by the depth-averaged concentration at a certain position. This can be more convenient since only two dimensions (instead of three) have to be taken into account. The concentration is not completely uniform over depth and can therefore be written as the sum of depth-averaged concentration $\tilde{c}$ and the vertical variation in concentration c'

$$c = \tilde{c} + c'$$

The time-averaged flows can be written as the sum of the depth-averaged velocity $\tilde{u}$ and the the variation from this average u'

$$u_1 = \tilde{u}_1 + u_1'$$
$$u_2 = \tilde{u}_2 + u_2'$$

Substituting this in equation 2.9, gives:

$$\frac{\partial \tilde{c}+c'}{\partial t} = -\frac{\partial(\tilde{u}_1+u_1')(\tilde{c}+c')}{\partial x_1} - \frac{\partial \tilde{u}_2+u_2'(\tilde{c}+c')}{\partial x_2} - \frac{\partial u_3(\tilde{c}+c')}{\partial x_3} + \frac{\partial}{\partial x_1}\left(k_1\frac{\partial \tilde{c}+c'}{\partial x_1}\right) + \frac{\partial}{\partial x_2}\left(k_2\frac{\partial \tilde{c}+c'}{\partial x_2}\right) + \frac{\partial}{\partial x_3}\left(k_3\frac{\partial \tilde{c}+c'}{\partial x_3}\right) \tag{2.10}$$

By integrating this equation over the depth, the following equation is obtained:

$$\frac{\partial H\tilde{c}}{\partial t} = -\frac{\partial H\tilde{u}_1\tilde{c}}{\partial x_1} - \frac{\partial H\tilde{u}_2\tilde{c}}{\partial x_2} - \frac{\partial H\overline{u_1'c'}}{\partial x_1} - \frac{\partial H\overline{u_2'c'}}{\partial x_2} + \frac{\partial}{\partial x_1}\left(k_1\frac{\partial \tilde{c}}{\partial x_1}\right) + \frac{\partial}{\partial x_2}\left(k_2\frac{\partial \tilde{c}}{\partial x_2}\right) \tag{2.11}$$

The $\overline{u_i'c'}$ represent the advective transport due to velocity variations in the vertical direction, these terms can also be represented as:

$$k_i H\frac{\partial \tilde{c}}{\partial x_i} + H\overline{u_i'C'} = -K_i H\frac{\partial \tilde{c}}{\partial x_i} \tag{2.12}$$

Substituting this and dropping the tildes gives as a final result the depth averaged advection-diffusion equation.

$$\frac{\partial Hc}{\partial t} = -\frac{\partial Hu_1c}{\partial x_1} - \frac{\partial Hu_2c}{\partial x_2} + \frac{\partial}{\partial x_1}\left(K_1H\frac{\partial c}{\partial x_1}\right) + \frac{\partial}{\partial x_2}\left(K_2H\frac{\partial c}{\partial x_2}\right) \tag{2.13}$$

For macroplastics it is even easier to transform equation 2.9 into a two dimensional advection-diffusion equation. Macroplastics are assumed to be floating, this means that there will be no concentration transport in the vertical direction and those terms can be set zero without further problems, this gives:

$$\frac{\partial c}{\partial t} = -\frac{\partial u_1c}{\partial x_1} - \frac{\partial u_2c}{\partial x_2} + \frac{\partial}{\partial x_1}\left(k_1\frac{\partial c}{\partial x_1}\right) + \frac{\partial}{\partial x_2}\left(k_2\frac{\partial c}{\partial x_2}\right) \tag{2.14}$$

Clearly this is a specific case of equation 2.13 (simply define $H = 1$). Therefore equation 2.13 will be used as general two dimensional advection-diffusion equation in the remainder of this report.

2.3. Numerical methods for solving the advection-diffusion equation

To simulate the transport of plastic particles, the advection-diffusion equation needs to be solved. Solving this equation analytically becomes quickly too complex, luckily there are various options to find a numerical solution. Over the years, there is a variety of different solving methods for the advection-diffusion equation developed. Most numerical solving methods can be divided into two fundamentally different approaches: the Eulerian and the Lagrangian approach.

2.3.1. Eulerian approach

The Eulerian approach solves the advection-diffusion equation on a fixed spatial grid, a fixed control volume is considered. This gives the advantages of a fixed spatial grid and it is easy to implement. A disadvantage of Eulerian methods is that when considering a problem with a high initial concentration, these methods can produce inaccurate and unrealistic solutions, for example negative concentrations or mass balance errors. The simulations of this report would have high initial concentrations, so the Eulerian approach was not preferred.

2.3.2. Lagrangian approach

The Lagrangian approach does not use a fixed spatial grid. Instead of solving the advection-diffusion equation directly, it models the motion of a large number of individual particles. By modelling the movement of many individual particles, the particle concentration can be obtained. In this report a Lagrangian method is used. A few advantages of the Lagrangian approach are that it is not necessary to solve the advection-diffusion equation directly and it also works for high initial concentrations. The Lagrangian method that will be used in this report is the random walk method. This method models the movement of a particle as a stochastic differential equation that is consistent with the advection-diffusion equation. The next chapter will therefore provide some necessary information about stochastic differential equations.

3

Stochastic differential equations

The previous chapter explained that the advection-diffusion equation needs to be solved to model the transport of plastic particles. This will be done using a Lagrangian approach where the movement of a large number of individual particles is simulated. The next chapter will show that the movement of one particle can be described with a stochastic differential equation. This chapter will give a brief overview of the necessary theory of stochastic differential equations.

3.1. Introduction to stochastic differential equations

To define a stochastic differential equation(SDE), some knowledge about stochastic processes is required. An important stochastic process is a Wiener process, it is the scaling limit of a random walk. This means that it is the same as a random walk with extremely small steps. The Wiener process is also similar to the physical phenomenon called Brownian motion. Brownian motion is the random movement of particles suspended in a fluid. The Wiener Process is defined as:

A standard Wiener process $W_t = (W_t, t \geq 0)$*, on* $[0, T]$ *is a process with* $W_0 = 0$ *and with stationary independent increments such that for any* $0 \leq s < t \leq T$*, the increment* $W_t - W_s$ *is a Gaussian random variable with mean zero and variance equal to* $t - s$*. That is,* $\mathbb{E}(W_t - W_s) = 0$*, and* $Var(W_t - W_s) = t - s$*.*

To define a SDE, Stochastic limits are needed. The definition of a stochastic limit is:

A row of stochastic variables X_n *converges in mean square sense to a limit* X *if:*

$$\lim_{n\to\infty} \mathbb{E}((X_n - X)^2) = 0$$

This can be written as

$$\text{l.i.m.}_{n\to\infty} X_n = X$$

With this knowledge, it is possible to define stochastic integrals. There are different definitions for Stochastic integrals. Here the Îto integral will be used, which is defined as follows:

$$\int_{t_0}^{t} G_s dW_s = \text{l.i.m.}_{h\to 0} \sum G_{t_i} (W_{t_{i=1}} - W_{t_i}) \tag{3.1}$$

G_s is a general stochastic process, W_s is a Wiener process and l.i.m. is the limit in mean square sense.

With this definition for stochastic integrals, it is possible to define a stochastic differential equation. The Îto stochastic differential equation can be defined as:

$$X_t = X_0 + \int_{t_0}^{t} f(X_s, s) ds + \int_{t_0}^{t} g(X_s, s) dW_s \tag{3.2}$$

or

$$dX_t = f(X_t, t) dt + g(X_t, t) dW_t \tag{3.3}$$

With the stochastic integral interpreted in Îto sense.

With a small time step the Îto stochastic differential equation can be solved numerically using the Euler scheme (Heemink [7]):

$$\begin{aligned} X_{t+\Delta t} &= X_t + \int_t^{t+\Delta t} f(X_s,s)ds + \int_t^{t+\Delta t} g(X_s,s)dW_s \approx X_t + \int_t^{t+\Delta t} f(X_t,t)ds + \int_t^{t+\Delta t} g(X_t,t)dW_s = \\ &= X_t + f(X_t,t)\Delta t + g(X_t,t)(W_{t+\Delta t} - W_t) \end{aligned} \tag{3.4}$$

3.2. Kolmogorov forward equation

For a better understanding of a stochastic process, it can be useful to know the evolution of the probability distribution of that process. The probability distribution of X_t in equation 3.3 can be obtained by solving the Kolmogorov forward equation, also know as the Fokker-Planck equation. If at a time s a particle is at position y, the Kolmogorov forward equation will give the probability distribution for the position of that particle at a future time $t > s$. So when the starting position of a particle is known, the solution of the Kolmogorov equation will be the probability distribution of the particle at time t. This can give a lot of information, for example where the particle will be likely to end up and what will be possible paths taken by this particle. The Kolmogorov forward equation is defined as:

$$\frac{\partial p(t,\mathbf{x}|s,\mathbf{y})}{\partial t} = -\sum_{i=1}^{n} \frac{\partial a_i(t,\mathbf{x})p(t,\mathbf{x}|s,\mathbf{y})}{\partial x_i} + \sum_{i=1}^{n}\sum_{j=1}^{n} \frac{\partial^2 b_{ij}(t,\mathbf{x})p(t,\mathbf{x}|s,\mathbf{y})}{\partial x_i \partial x_j} \tag{3.5}$$

with

$$t_0 \le t \le T$$

$$p(t=s,\mathbf{x}|s,\mathbf{y}) = \delta(\mathbf{x}-\mathbf{y})$$

a_i are often called drift terms and b_{ij} are diffusion terms. b_{ij} is a symmetric and positive definite matrix:

$$b_{ij} = \frac{1}{2}(\sigma\sigma^T)_{ij} \tag{3.6}$$

As said, the solution of the Kolmogorov forward equation p, is a probability distribution. So it gives the probability a particle is found at position $\mathbf{x}$ at time t, given it was at position $\mathbf{y}$ at time s.

To derive the Kolmogorov forward equation, Îto's differentiation rule is needed. This rule is defined as:
Let X_t be the unique solution of the Îto SDE:

$$dX_t = f(X_t,t)dt + g(X_t,t)dW_t$$

Let $\phi(x,t)$ be a scalar valued real function continuously differentiable in t and having continuous second partial derivatives with respect to x, then the SDE for $\phi(x,t)$ is:

$$d\phi = \frac{\partial\phi}{dt}dt + \frac{\partial\phi}{dx}dX_t + \frac{1}{2}g^2\frac{\partial^2\phi}{\partial x^2}dt$$

As done in Heemink [7], here is shown how the Kolmogorov equation can be derived in one dimension using a Kernel function $K(x)$ and Îto's differentiation rule. Start with applying Îto's differential rule on $\phi(x,t) = K(x)$

$$dK(X_t) = \frac{\partial K}{\partial x}dX_t + \frac{1}{2}g(X_t,t)^2\frac{\partial^2 K}{\partial x^2}dt \tag{3.7}$$

Fill in the definition of dX_t:

$$dK(X_t) = \frac{\partial K}{\partial x}(f(X_t,t)dt + g(X_t,t)dW_t) + \frac{1}{2}g(X_t,t)^2\frac{\partial^2 K}{\partial x^2}dt \tag{3.8}$$

Taking the expectation gives:

$$\frac{d\mathbb{E}(K(X_t))}{dt} = \mathbb{E}\left(\frac{\partial K}{\partial x}f(X_t) + \frac{1}{2}g(X_t,t)^2\frac{\partial^2 K}{\partial x^2}\right) \tag{3.9}$$

Using the probability density function of X_t, this expression can be rewritten as:

$$\frac{d}{dt}\int_{-\infty}^{\infty} K(x)p(x,t)dx = \int_{-\infty}^{\infty} \frac{\partial K}{\partial x} f(x,t)p(x,t)dx + \int_{-\infty}^{\infty} \frac{1}{2} g(x,t)^2 \frac{\partial^2 K}{\partial x^2} p(x,t)dx \tag{3.10}$$

Partial integration and using that the Kernel function is 0 at $\pm\infty$, results in:

$$\int_{-\infty}^{\infty} K(x)\frac{\partial p(x,t)}{\partial t}dx = \int_{-\infty}^{\infty} -K(x)\frac{\partial f(x,t)p(x,t)}{\partial x}dx + \int_{-\infty}^{\infty} K(x)\frac{1}{2}\frac{\partial^2 g(x,t)^2 p(x,t)}{\partial x^2}dx \tag{3.11}$$

Which is the same as:

$$\int_{-\infty}^{\infty} K(x)\left(\frac{\partial p(x,t)}{\partial t} + \frac{\partial f(x,t)p(x,t)}{\partial x} - \frac{1}{2}\frac{\partial^2 g(x,t)^2 p(x,t)}{\partial x^2}\right)dx = 0 \tag{3.12}$$

This means that:

$$\frac{\partial p(x,t)}{\partial t} + \frac{\partial f(x,t)p(x,t)}{\partial x} - \frac{1}{2}\frac{\partial^2 g(x,t)^2 p(x,t)}{\partial x^2} = 0 \tag{3.13}$$

Defining $f(x,t) = a(x,t)$ and $g(x,t) = \sigma(x,t)$ and using 3.6 gives:

$$\frac{\partial p(x,t)}{\partial t} = -\frac{\partial a(x,t)p(x,t)}{\partial x} + \frac{\partial^2 b(x,t)p(x,t)}{\partial x^2} \tag{3.14}$$

Since the above derivation holds for any Kernel function, the Kolmogorov forward equation in one dimension is obtained. This can easily be generalised for more dimensions to get equation 3.5. For n dimensions the Kolmogorov forward equation can also be written as:

$$\frac{\partial p(t,\mathbf{x}|s,\mathbf{y})}{\partial t} + \mathscr{L}p(t,\mathbf{x}|s,\mathbf{y}) = 0 \tag{3.15}$$

With

$$\mathscr{L}(\cdot) = \sum_{i=1}^{n}\sum_{j=1}^{n} \frac{\partial a(t,x)(\cdot)}{\partial x_i} - \frac{\partial^2 b(t,x)(\cdot)}{\partial x_i \partial x_j}$$

3.3. Kolmogorov backward equation

Instead of finding out how a process will evolve over time, it can also be useful to know what has happened before. To find out where a particle came from, one could use forward simulations on a large number of different positions to see with what probability the particle would end up at the given point. However this would be very time consuming and unnecessary complex. Instead, the Kolmogorov backwards equation could be used to obtain a probability distribution of the origin of this particle. The Kolmogorov backwards equation gives the reverse time evolution of a stochastic process X_t and it is the adjoint of the Kolmogorov forward equation. When a particle is found at position $\mathbf{x}$ and time t, the solution of the Kolmogorov backward equation is the probability distribution for $s < t$. This means it will give the probability a particle was located at position $\mathbf{y}$ at time $s < t$ when the particle is found at position $\mathbf{x}$ at time t. In other words, solving this equation will give the origin and possible taken paths of a particle. The Kolmogorov backward equation can be written as:

$$\frac{\partial \tilde{p}(t,\mathbf{x}|s,\mathbf{y})}{\partial s} + \mathscr{L}^{\dagger}\tilde{p}(t,\mathbf{x}|s,\mathbf{y}) = 0 \tag{3.16}$$

To find $\mathscr{L}^{\dagger}$, the adjoint of $\mathscr{L}$ needs to be calculated. The definition for an adjoint states for all suitable functions f and g that:

$$\langle f, \mathscr{L}g\rangle = \langle \mathscr{L}^{\dagger}f, g\rangle \tag{3.17}$$

Using the definition of the inner product for continuous functions, this means that:

$$\int_{-\infty}^{\infty} f(t,\mathbf{x}|s,\mathbf{y})\mathscr{L}(g(t,\mathbf{x}|s,\mathbf{y}))dx = \int_{-\infty}^{\infty} g(t,\mathbf{x}|s,\mathbf{y})\mathscr{L}^{\dagger}(f(t,\mathbf{x}|s,\mathbf{y}))dx \tag{3.18}$$

Here is shown how to derive the the adjoint of $\mathscr{L}$ in one dimension. Start by filling in the expression for $\mathscr{L}$ as defined in the previous section:

$$\int_{-\infty}^{\infty} f(t,x)\mathscr{L}(g(t,x))dx = \int_{-\infty}^{\infty} f(t,x)\left(\frac{\partial a(t,x)g(t,x)}{\partial x} - \frac{\partial^2 b(t,x)g(t,x)}{\partial x^2}\right)dx \tag{3.19}$$

This can also be written as:

$$\int_{-\infty}^{\infty} f(t,x)\mathscr{L}(g(t,x))dx = \int_{-\infty}^{\infty} f(t,x)(\frac{\partial a(t,x)g(t,x)}{\partial x}dx - \int_{-\infty}^{\infty} f(t,x)\frac{\partial^2 b(t,x)g(t,x)}{\partial x^2})dx \tag{3.20}$$

Calculate the two integrals on the right side separately. Use partial integration to see that the first integral results in:

$$\int_{-\infty}^{\infty} f(t,x)\frac{\partial a(t,x)g(t,x)}{\partial x}dx = \left[f(t,x)a(t,x)g(t,x)\right]_{-\infty}^{+\infty} - \int_{-\infty}^{\infty}\frac{\partial f(t,x)}{\partial x}a(t,x)g(t,x)dx \tag{3.21}$$

Since both density functions are 0 at $\pm\infty$, this equals:

$$\int_{-\infty}^{\infty} f(t,x)\frac{\partial a(t,x)g(t,x)}{\partial x}dx = -\int_{-\infty}^{\infty} g(t,x)a(t,x)\frac{\partial f(t,x)}{\partial x}dx \tag{3.22}$$

Now the second integral can be calculated. Use partial integration twice and use that the density functions are 0 at $\pm\infty$. This results in:

$$\int_{-\infty}^{\infty} f(t,x)\frac{\partial^2 b(t,x)g(t,x)}{\partial x^2})dx = \int_{-\infty}^{\infty} g(t,x)b(t,x)\frac{\partial^2 f(t,x)}{\partial x^2}dx \tag{3.23}$$

Now the result of the two integrals can be combined to:

$$\int_{-\infty}^{\infty} f(t,x)\mathscr{L}(g(t,x))dx = -\int_{-\infty}^{\infty} g(t,x)a(t,x)\frac{\partial f(t,x)}{\partial x}dx - \int_{-\infty}^{\infty} g(t,x)b(t,x)\frac{\partial^2 f(t,x)}{\partial x^2}dx \tag{3.24}$$

This is the same as:

$$\int_{-\infty}^{\infty} f(t,x)\mathscr{L}(g(t,x))dx = \int_{-\infty}^{\infty} -g(t,x)a(t,x)\frac{\partial f(t,x)}{\partial x} - g(t,x)b(t,x)\frac{\partial^2 f(t,x)}{\partial x^2}dx \tag{3.25}$$

Which means that:

$$\int_{-\infty}^{\infty} f(t,x)\mathscr{L}(g(t,x))dx = \int_{-\infty}^{\infty} g(t,x)\left(-a(t,x)\frac{\partial f(t,x)}{\partial x} - b(t,x)\frac{\partial^2 f(t,x)}{\partial x^2}\right)dx = \int_{-\infty}^{\infty} g(t,x)\mathscr{L}^{\dagger}(f(t,x))dx \tag{3.26}$$

Last the coordinates x and t are changed to s and y, $\mathscr{L}^{\dagger}$ can now be defined as:

$$\mathscr{L}^{\dagger}(\cdot) = a(s,y)\frac{\partial(\cdot)}{\partial y} + b(s,y)\frac{\partial^2(\cdot)}{\partial y^2} \tag{3.27}$$

Substituting this into equation 3.16, leads to the Kolmogorov backward equation in one dimension:

$$\frac{\partial\tilde{p}(t,x|s,y)}{\partial s} = -a(s,y)\frac{\partial\tilde{p}(t,x|s,y)}{\partial y} - b(s,y)\frac{\partial^2\tilde{p}(t,x|s,y)}{\partial y^2} \tag{3.28}$$

This derivation can easily be generalised for more dimensions, which gives the Kolmogorov backward equation for n dimensions:

$$\frac{\partial\tilde{p}(t,\mathbf{x}|s,\mathbf{y})}{\partial s} = -\sum_{i=1}^{n} a_i(s,\mathbf{y})\frac{\partial\tilde{p}(t,\mathbf{x}|s,\mathbf{y})}{\partial y_i} - \sum_{i=1}^{n}\sum_{j=1}^{n} b_{ij}(s,\mathbf{y})\frac{\partial^2\tilde{p}(t,\mathbf{x}|s,\mathbf{y})}{\partial y_i\partial y_j} \tag{3.29}$$

4

Relation between transport models and stochastic differential equations

In chapter 2 the advection-diffusion equation was derived and in chapter 3 the Kolmogorov equations were obtained. Now the connection between these equations will be shown as well as how to solve them using a Lagrangian approach. At the end of this chapter more information will be given about the drift and diffusion terms used in the Kolmogorov equations.

4.1. Advection-diffusion equation and Kolmogorov forward equation

The Kolmogorov forward equation can be transformed into the advection-diffusion equation. This means that a solution of the Kolmogorov equation should also be a solution of the advection-diffusion equation. This section will show how the advection-diffusion equation can be rewritten as Kolmogorov forward equation in a few steps. As seen in section 2.2, the depth averaged advection-diffusion equation is defined as:

$$\frac{\partial Hc}{\partial t} = \sum_{i=1}^{2}\sum_{j=1}^{2} -\frac{\partial u_i Hc}{\partial x_i} + \frac{\partial}{\partial x_i}\left(k_{ij} H \frac{\partial c}{\partial x_j}\right) \tag{4.1}$$

With $c(x,t)$ a concentration field and $H(x,t)$ the water depth. Now start by writing the advection-diffusion equation as:

$$\frac{\partial Hc}{\partial t} = \sum_{i=1}^{2}\sum_{j=1}^{2} -\frac{\partial u_i Hc}{\partial x_i} + \frac{\partial}{\partial x_i}\left(\frac{\partial k_{ij} Hc}{\partial x_j} - c\frac{\partial k_{ij} H}{\partial x_j}\right) \tag{4.2}$$

Rearrange the terms:

$$\frac{\partial Hc}{\partial t} = \sum_{i=1}^{2}\sum_{j=1}^{2} -\frac{\partial}{\partial x_i}\left(u_i Hc + c\frac{\partial k_{ij} H}{\partial x_j}\right) + \frac{\partial^2 k_{ij} Hc}{\partial x_i \partial x_j} \tag{4.3}$$

Which is the same as:

$$\frac{\partial Hc}{\partial t} = \sum_{i=1}^{2}\sum_{j=1}^{2} -\frac{\partial}{\partial x_i}\left(u_i Hc + Hc\frac{\partial k_{ij}}{\partial x_j} + ck_{ij}\frac{\partial H}{\partial x_j}\right) + \frac{\partial^2 k_{ij} Hc}{\partial x_i \partial x_j} \tag{4.4}$$

This can be written as:

$$\frac{\partial Hc}{\partial t} = \sum_{i=1}^{2}\sum_{j=1}^{2} -\frac{\partial}{\partial x_i}\left(\left(u_i + \frac{\partial k_{ij}}{\partial x_j} + \frac{k_{ij}}{H}\frac{\partial H}{\partial x_j}\right) Hc\right) + \frac{\partial^2 k_{ij} Hc}{\partial x_i \partial x_j} \tag{4.5}$$

Now assume:

$$\begin{aligned} a_i &= u_i + \tfrac{\partial k_{ij}}{\partial x_j} + \tfrac{k_{ij}}{H}\tfrac{\partial H}{\partial x_j} \\ b_{ij} &= k_{ij} \\ c(x,t) &= \tfrac{p(x,t)}{H} \end{aligned} \tag{4.6}$$

Filling this in, will yield the Kolmogorov forward equation for 2 dimensions:

$$\frac{\partial p}{\partial t} = \sum_{i=1}^{2}\sum_{j=1}^{2} -\frac{\partial a_i p}{\partial x_i} + \frac{\partial^2 b_{ij} p}{\partial x_i \partial x_j} \tag{4.7}$$

The drift term a_i now includes two extra terms. The extra terms are a correction necessary when there is a spatially varying diffusivity and/or water depth. Section 4.4 will further elaborate on the drift term and this correction velocity.

4.2. Lagrangian approach for advection-diffusion equation

The advection-diffusion equation (equation 4.1) can be solved using the Lagrangian random walk model (Heemink [7]). This method will model the movement of a large number of individual particles to obtain the solution of the advection-diffusion equation. The movement of the individual particles will be described by stochastic differential equations that are consistent with the advection-diffusion equation. To find these SDEs, the advection-diffusion equation is interpreted as the Kolmogorov forward equation. The Kolmogorov forward equation will be replaced with Îto SDEs for the position of one particle using Îto's differentiation rule as defined in the previous chapter. The Îto SDEs that will replace equation 4.1 are:

$$\begin{aligned} dX(t) &= a_x(t)dt + \sigma(X,t)dW_x(t) \\ dY(t) &= a_y(t)dt + \sigma(Y,t)dW_y(t) \end{aligned} \tag{4.8}$$

with $W_x(t)$ and $W_y(t)$ two independent Wiener processes.

Îto Stochachstic Differential Equations can be solved numerically using the Euler scheme (Heemink [7]). The numerical solution of equation 4.8 is:

$$\begin{aligned} X(t+\triangle t) &= X(t) + a_x(t)\triangle t + \sigma(X,t)(W_x(t+\triangle t) - W_x(t)) \\ Y(t+\triangle t) &= Y(t) + a_y(t)\triangle t + \sigma(Y,t)(W_y(t+\triangle t) - W_y(t)) \\ X(0) &= x_0, Y(0) = y_0 \end{aligned} \tag{4.9}$$

These equations will be used to simulate the position of a large number of individual particles. The distribution of those particles equals the probability distribution that would solve the Kolmogorov forward equation. These results could then be used to produce a risk map to indicate in which areas the probability to find plastic particles is high.

4.3. Lagrangian approach for reverse time advection-diffusion equation

At the end of the previous chapter the Kolmogorov backward equation was obtained. This equation can be solved in a similar way as the Kolmogorov forward equation. To solve the Kolmogorov backward equation in this way, it should first be rewritten into the same form as the Kolmogorov forward equation. How this can be done, is shown here for n dimensions (Syed [16]).

Start with the Kolmogorov backward equation as derived in the previous chapter:

$$\frac{\partial \tilde{p}}{\partial s} = -\sum_{i=1}^{n} a_i \frac{\partial \tilde{p}}{\partial y_i} - \sum_{i=1}^{n}\sum_{j=1}^{n} b_{ij}\frac{\partial^2 \tilde{p}}{\partial y_i \partial y_j} \tag{4.10}$$

Which is the same as:

$$\frac{\partial \tilde{p}}{\partial s} = -\sum_{i=1}^{n} a_i \frac{\partial \tilde{p}}{\partial y_i} - \sum_{i=1}^{n}\sum_{j=1}^{n}\left(\frac{\partial^2 b_{ij}\tilde{p}}{\partial y_i \partial y_j} - \tilde{p}\frac{\partial^2 b_{ij}}{\partial y_i \partial y_j} - \frac{\partial b_{ij}}{\partial y_i}\frac{\partial \tilde{p}}{\partial y_j} - \frac{\partial b_{ij}}{\partial y_j}\frac{\partial \tilde{p}}{\partial y_i}\right) \tag{4.11}$$

Since b_{ij} is symmetric, this can be rewritten as:

$$\frac{\partial \tilde{p}}{\partial s} = -\sum_{i=1}^{n} a_i \frac{\partial \tilde{p}}{\partial y_i} - \sum_{i=1}^{n}\sum_{j=1}^{n}\left(\frac{\partial^2 b_{ij}\tilde{p}}{\partial y_i \partial y_j} - \tilde{p}\frac{\partial^2 b_{ij}}{\partial y_i \partial y_j} - 2\frac{\partial b_{ij}}{\partial y_j}\frac{\partial \tilde{p}}{\partial y_i}\right) \tag{4.12}$$

Rearranging some of the terms gives:

$$\frac{\partial \tilde{p}}{\partial s} = \sum_{i=1}^{n}\sum_{j=1}^{n}\left(-a_i \frac{\partial \tilde{p}}{\partial y_i} - \frac{\partial^2 b_{ij}\tilde{p}}{\partial y_i \partial y_j} + \tilde{p}\frac{\partial^2 b_{ij}}{\partial y_i \partial y_j} + 2\frac{\partial b_{ij}}{\partial y_j}\frac{\partial \tilde{p}}{\partial y_i}\right) \tag{4.13}$$

$$\frac{\partial \tilde{p}}{\partial s} = \sum_{i=1}^{n}\sum_{j=1}^{n}\left(\left(-a_i + 2\frac{\partial b_{ij}}{\partial y_j}\right)\frac{\partial \tilde{p}}{\partial y_i} - \frac{\partial^2 b_{ij}\tilde{p}}{\partial y_i \partial y_j} + \tilde{p}\frac{\partial^2 b_{ij}}{\partial y_i \partial y_j}\right) \tag{4.14}$$

For divergence-free flow, it is true that:

$$\frac{\partial}{\partial y_i}\left(a_i - \frac{\partial b_{ij}}{\partial y_j}\right) = 0 \tag{4.15}$$

Which means that:

$$\frac{\partial}{\partial y_i}\left(\left(a_i - \frac{\partial b_{ij}}{\partial y_j}\right)\tilde{p}\right) = \left(a_i - \frac{\partial b_{ij}}{\partial y_j}\right)\frac{\partial \tilde{p}}{\partial y_i} \tag{4.16}$$

This can be used to rewrite the equation as:

$$\frac{\partial \tilde{p}}{\partial s} = \sum_{i=1}^{n}\sum_{j=1}^{n}\frac{\partial \tilde{a}_i \tilde{p}}{\partial y_i} - \frac{\partial^2 b_{ij}\tilde{p}}{\partial y_i \partial y_j} + \tilde{p}\frac{\partial^2 b_{ij}}{\partial y_i \partial y_j} \tag{4.17}$$

with

$$\tilde{a}_i = -a_i + 2\frac{\partial b_{ij}}{\partial y_j} \tag{4.18}$$

Now an equation is obtained that can be solved with the same method as used for the Kolmogorov forward equation. This equation can also be transformed into a reverse time advection-diffusion equation. This will also be shown, start by filling in $\tilde{p} = H\tilde{c}$ in the two dimensional equation:

$$\frac{\partial H\tilde{c}}{\partial s} = \sum_{i=1}^{2}\sum_{j=1}^{2}\frac{\partial \tilde{a}_i H\tilde{c}}{\partial y_i} - \frac{\partial^2 b_{ij}H\tilde{c}}{\partial y_i \partial y_j} + H\tilde{c}\frac{\partial^2 b_{ij}}{\partial y_i \partial y_j} \tag{4.19}$$

Next, rewrite the second term on the right side of the equation:

$$\frac{\partial H\tilde{c}}{\partial s} = \sum_{i=1}^{2}\sum_{j=1}^{2}\frac{\partial \tilde{a}_i H\tilde{c}}{\partial y_i} - \frac{\partial}{\partial y_i}\left(b_{ij}H\frac{\partial \tilde{c}}{\partial y_j} + \tilde{c}\frac{\partial b_{ij}H}{\partial y_j}\right) + H\tilde{c}\frac{\partial^2 b_{ij}}{\partial y_i \partial y_j} \tag{4.20}$$

Now the terms can be rearranged:

$$\frac{\partial H\tilde{c}}{\partial s} = \sum_{i=1}^{2}\sum_{j=1}^{2}\frac{\partial}{\partial y_i}\left(\tilde{a}_i H\tilde{c} - \frac{\partial b_{ij}H}{\partial y_j}\tilde{c}\right) - \frac{\partial}{\partial y_i}\left(b_{ij}H\frac{\partial \tilde{c}}{\partial y_j}\right) + H\tilde{c}\frac{\partial^2 b_{ij}}{\partial y_i \partial y_j} \tag{4.21}$$

$$\frac{\partial H\tilde{c}}{\partial s} = \sum_{i=1}^{2}\sum_{j=1}^{2}\frac{\partial}{\partial y_i}\left(\tilde{a}_i H\tilde{c} - \frac{\partial b_{ij}}{\partial y_j}H\tilde{c} - \frac{\partial H}{\partial y_j}b_{ij}\tilde{c}\right) - \frac{\partial}{\partial y_i}\left(b_{ij}H\frac{\partial \tilde{c}}{\partial y_j}\right) + H\tilde{c}\frac{\partial^2 b_{ij}}{\partial y_i \partial y_j} \tag{4.22}$$

$$\frac{\partial H\tilde{c}}{\partial s} = \sum_{i=1}^{2}\sum_{j=1}^{2}\frac{\partial}{\partial y_i}\left(\left(\tilde{a}_i - \frac{\partial b_{ij}}{\partial y_j} - \frac{b_{ij}}{H}\frac{\partial H}{\partial y_j}\right)H\tilde{c}\right) - \frac{\partial}{\partial y_i}\left(b_{ij}H\frac{\partial \tilde{c}}{\partial y_j}\right) + H\tilde{c}\frac{\partial^2 b_{ij}}{\partial y_i \partial y_j} \tag{4.23}$$

Filling in

$$\tilde{u_i} = \tilde{a}_i - \frac{\partial b_{ij}}{\partial y_j} - \frac{b_{ij}}{H}\frac{\partial H}{\partial y_j} = -a_i + \frac{\partial b_{ij}}{\partial y_j} - \frac{b_{ij}}{H}\frac{\partial H}{\partial y_j}$$

and

$$b_{ij} = k_{ij}$$

results in a reverse time advection-diffusion equation:

$$\frac{\partial H\tilde{c}}{\partial s} = \sum_{i=1}^{2}\sum_{j=1}^{2}\frac{\partial \tilde{u}_i H\tilde{c}}{\partial y_i} - \frac{\partial}{\partial y_i}\left(k_{ij}\frac{\partial H\tilde{c}}{\partial y_j}\right) + H\tilde{c}\frac{\partial^2 k_{ij}}{\partial y_i \partial y_j} \tag{4.24}$$

To solve this reverse time advection-diffusion equation, the approach will be the same as for solving the forward equation. Again the advection-diffusion equation is interpreted as the Kolmogorov equation (equation 4.17), which can be replaced by a system of SDEs. However, equation 4.17 has some extra terms compared to the forward equation. Consequently solving this equation is slightly different. An extra equation

is added to the system of SDEs to make is consistent with the Kolmogorov backward equation (Spivakovs'ka [15]):

$$\begin{aligned} dX(s) &= \tilde{a}_x(s)\cdot ds + \sigma(X,s)dW_x(s) \\ dY(s) &= \tilde{a}_y(s)\cdot ds + \sigma(Y,s)dW_y(s) \\ d\mathcal{Z} &= \left(\frac{\partial^2 b_{xx}}{\partial x^2} + \frac{\partial^2 b_{xy}}{\partial x \partial y} + \frac{\partial^2 b_{yy}}{\partial y^2} + \frac{\partial^2 b_{yx}}{\partial y \partial x}\right)\mathcal{Z}\,ds \end{aligned} \tag{4.25}$$

This system of SDE's can again be solved with the Euler scheme, this results in:

$$\begin{aligned} X(s+\triangle s) &= X(s) + \tilde{a}_x(s)\triangle s + \sigma(X,s)(W_x(s+\triangle s) - W_x(s)) \\ Y(s+\triangle s) &= Y(s) + \tilde{a}_y(s)\triangle s + \sigma(Y,s)(W_y(s+\triangle s) - W_y(s)) \\ \mathcal{Z}(s+\triangle s) &= \mathcal{Z}(s) + \left(\frac{\partial^2 b_{xx}}{\partial x^2} + \frac{\partial^2 b_{xy}}{\partial x \partial y} + \frac{\partial^2 b_{yy}}{\partial y^2} + \frac{\partial^2 b_{yx}}{\partial y \partial x}\right)\mathcal{Z}(s)\triangle s \\ X(0) &= x_0, Y(0) = y_0, \mathcal{Z}(0) = 1 \end{aligned} \tag{4.26}$$

$\mathcal{Z}$ can be seen as a kind of weighing function. When a particle has a high weight, the chance is higher that a particle was released at that position. In other words, the particles with a higher weight are 'more important' for the probability distribution. After simulating for a large amount of particles, a risk map can be made using the positions and weights of the simulated particles.

4.4. Drift and diffusion term

It should be clear now which equations can describe the movement of plastic particles and how these equation can be solved. However, for realistic results the correct values for a and σ should be chosen. Therefore it is necessary to know what is affecting the drift term **a** and diffusion term **b** of the Kolmogorov equations.

4.4.1. Drift term for macroplastics

The drift term (**a** in the Kolmogorov equations) can be interpreted as the velocity of the particles. Macroplastics are assumed to be floating on the water, so the drift term is determined by the water velocity **u** and the wind velocity **v**:

$$\mathbf{a}(a,y,t) = \mathbf{u}(x,y,t) + \alpha\mathbf{v}(x,y,t) \tag{4.27}$$

Here α is the wind drift coefficient, which is dimensionless. It is a value for the influence of the drag force of the wind on the object. The value for the wind drift coefficient is depending on the buoyancy, shape and size of the macroplastic in the water. α is defined as:

$$\alpha = \sqrt{\frac{\rho_a A_a C d_a}{\rho_w A_w C d_w}} \tag{4.28}$$

ρ_a and ρ_w are the densities of respectively air and water, A_a and A_w are the cross sectional areas of the macroplastic affected by the wind and water and Cd_a and Cd_w are the drag coefficients of the part of the macroplastic that is in the air and water (Hardesty and Wilcox [6]).

This means that α can vary a lot depending on the size, form and weight of the macroplastic. For the simulations in this report a value of 0.03 was chosen. This is the wind drift coefficient for a particle that is half in the water and half above the water and with drag coefficients of the part in the water and above the water being equal.

4.4.2. Drift term for microplastics

For microplastics the definition of the drift term is different because the microplastics are spread through the water column instead of floating on the water. Consequently, microplastics are not affected by the wind. This does not mean that the drift term is only depending on the current though. For microplastics a correction related to the bathymetry gradient is necessary, this is the second term in the definition of the drift term for microplastics:

$$\mathbf{a}(x,y,t) = \mathbf{u}(x,y,t) + \kappa(x,y,t)\frac{\nabla H(x,y,t)}{H(x,y,t)} \tag{4.29}$$

Here κ is the diffusivity $[m^2/s]$ and H is the water depth (the distance from the water surface to the sea floor in metres).

The correction related to bathymetry gradient is found when the depth-average advection-diffusion equation is transformed into the Kolmogorov equation, as was shown in section 4.1. The resulting definition for a_i was:

$$a_i = u_i + \frac{\partial k_{ij}}{\partial x_j} + \frac{k_{ij}}{H}\frac{\partial H}{\partial x_j} \tag{4.30}$$

When H and κ are constant the drift term is simply equal to the water velocity. However when the water depth and/or diffusivity are varying in space, it is necessary to add a correction velocity to the drift term, equal to $\tilde{u} = \frac{\partial k_{ij}}{\partial x_j} + \frac{k_{ij}}{H}\frac{\partial H}{\partial x_j}$. This correction velocity tends to transports particles towards regions of increasing depth and diffusivity. Without the correction velocity the movement of particles would be biased to regions with a lower water depth and diffusivity (Hunter et al. [9], Spagnol et al. [14]).

Imagine microplastics in water with a spatially varying diffusivity so that there is an area with a large diffusivity surrounded by an area with a small diffusivity. In time the concentration of particles should become homogeneous over the whole region. However, particles in the area with a high diffusivity move with a large random walk step size quickly away from this area but particles in the area with a low diffusivity can, due to their small random walk step size, only slowly move towards the area with high diffusivity. This would lead to a lower concentration in the area with high diffusivity. The correction velocity in the direction of increasing diffusivity can solve this problem.

Now imagine microplastics in water with a spatially varying water depth and a diffusivity (either constant or varying in space). After a while the particles should be spread homogeneous through the whole region. This means that a column with a high water depth should contain more particles than a column with a low water depth. However, since the particles are moving with a random walk in only two directions, this would mean that after a while each water column would contain the same amount of particles, regardless the water depth. To solve this, a correction moving particles towards areas with increasing water depth is necessary. One can see that this correction in not only defined by the spatial derivative of the water depth but also multiplied with the diffusivity and divided by the water depth. This way the correction velocity is proportional with the random walk step size.

In section 6.1, the necessity of this correction velocity is also shown with some simplified simulations for a space varying water depth. The correction for a spatially varying diffusivity ($\frac{\partial k_{ij}}{\partial x_i}$) is not necessary in the the drift term of this report because the diffusivity is defined constant. The diffusivity will be discussed further in the next section.

4.4.3. Diffusion term

The diffusion term (**b** in the Kolmogorov equations) indicates the degree of dispersion. It affects how much of a particles movement is random. The definition of the diffusion term is the same for both the micro- and macroplastics and equal to the diffusivity $\boldsymbol{\kappa}$:

$$\mathbf{b}(x, y, t) = \boldsymbol{\kappa}(x, y, t) \tag{4.31}$$

In Chapter 3, **b** was already defined to be a symmetric and positive definite matrix, this meant that:

$$\mathbf{b}(x, y, t) = \frac{1}{2}\boldsymbol{\sigma}\boldsymbol{\sigma}^T \tag{4.32}$$

From these definitions, it follows that:

$$\boldsymbol{\sigma}(x, y, t) = \sqrt{2\boldsymbol{\kappa}(x, y, t)} \tag{4.33}$$

Unfortunately the process of oceanic dispersion is complex and at this moment hardly any single theory can explain or interpret it fully. Empirical data can be used to find a suitable value for $\boldsymbol{\kappa}$. These empirical data are mostly collected by tracer experiments. An example of tracer experiments is releasing dye in the water and over time measuring the difference between the size of the patch and the initial patch. With this data the diffusivity can be computed (Okubo [13]). Another example of a tracer experiment is using Magnetically Attractive Particles(MAPs), composed of hollow glass to give them buoyancy. A large number of MAPs is released and

over time collected by a magnetic collector. This system is especially suitable to measure long-range dispersion and compare this with virtual particle dispersion estimates provided by hydrodynamic models (Hrycik et al. [8]).

It can be concluded that deciding on a suitable value for $\boldsymbol{\kappa}$ is not straightforward. When you know the velocity field of the area your simulating extremely well, $\boldsymbol{\kappa}$ can also be defined lower than with a less exact velocity field. To make it more complex, $\boldsymbol{\kappa}$ probably varies in space and time too. Since it was already questionable which empirical data for $\boldsymbol{\kappa}$ was most suitable, it was kept a constant in the simulations of this report. Varying $\boldsymbol{\kappa}$ would neither give better results nor more insight in the model. In Critchell et al. [3] and Critchell et al. [5] a standard value of 10 m^2/s was assumed based on several models and tracer experiments in the Great Barrier Reef. Since this model is based on Critchell et al. [5] the same value for κ was chosen for the simulations of this report even though the situation for these simulations is quite different.

5

Settling of particles

Particles that are moving through the water have a chance to sink and settle on the bottom of the ocean. There are various processes that can lead to settling, for example degradation, absorbing water or other substances and biofouling (a layer of micro-organisms accumulating on the surface). In this chapter two different methods are used to obtain an advection-diffusion equation that includes the settling of particles. Again the Lagrangian 'random walk' method will be used to solve this equation. Next the reverse time advection-diffusion equation that includes the settling is derived by finding the adjoint of the settling term, this equation will also be solved using a Lagrangian approach.

5.1. Settling of particles in advection-diffusion equation

Two different methods are used to add the settling of plastic particles to the advection-diffusion equation.

5.1.1. Method 1

This method is based on Charles [2]. Since every particle is either floating/suspended in the water or settled, a binary state can be assigned to every particle at time t:

$$S_t = \begin{cases} 1 & \text{particle is in suspention/floating} \\ 0 & \text{otherwise (particle is settled)} \end{cases} \tag{5.1}$$

Next a mass density can be defined for particles at position $\mathbf{x}$ and time t in terms of the probability density p and the chance that a particle does not settle $\mathbb{P}(S_t = 1)$:

$$\langle m(\mathbf{x}, t)\rangle = p(\mathbf{x}, t)\mathbb{P}(S_t = 1) \tag{5.2}$$

The above defined $\langle m\rangle$ can be differentiated to t

$$\frac{\partial\langle m\rangle}{\partial t} = \mathbb{P}(S_t = 1)\frac{\partial p}{\partial t} + p\frac{\partial\mathbb{P}(S_t = 1)}{\partial t} \tag{5.3}$$

Now the term $\frac{\partial p}{\partial t}$ can be replaced by the Fokker-Planck equation (equation 3.5).

$$\frac{\partial\langle m\rangle}{\partial t} = \mathbb{P}(S_t = 1)\left(-\sum_{i=1}^{n}\frac{\partial a_i p}{\partial x_i} + \sum_{i=1}^{n}\sum_{j=1}^{n}\frac{\partial^2 b_{ij} p}{\partial x_i \partial x_j}\right) + p\frac{\partial\mathbb{P}(S_t = 1)}{\partial t} \tag{5.4}$$

Since $\mathbb{P}$ is independent of position $\mathbf{x}$, this can be rewritten as:

$$\frac{\partial\langle m\rangle}{\partial t} = \sum_{i=1}^{n}\sum_{j=1}^{n} -\frac{\partial a_i p\mathbb{P}(S_t = 1)}{\partial x_i} + \frac{\partial^2 b_{ij} p\mathbb{P}(S_t = 1)}{\partial x_i \partial x_j} + p\frac{\partial\mathbb{P}(S_t = 1)}{\partial t} \tag{5.5}$$

Replacing $p(\mathbf{x}, t)\mathbb{P}(S_t = 1)$ by $\langle m\rangle$ gives:

$$\frac{\partial\langle m\rangle}{\partial t} = \sum_{i=1}^{n}\sum_{j=1}^{n} -\frac{\partial a_i\langle m\rangle}{\partial x_i} + \frac{\partial^2 b_{ij}\langle m\rangle}{\partial x_i \partial x_j} + p\frac{\partial\mathbb{P}(S_t = 1)}{\partial t} \tag{5.6}$$

Which looks like the Fokker-Planck equation again, with one extra term. Depending on the definition of $\mathbb{P}$ the term $\frac{\partial \mathbb{P}}{\partial t}$ can also be rewritten. Here we define $\frac{d\mathbb{P}}{dt} = -\gamma(x,t)\mathbb{P}$. This results into:

$$\frac{\partial \langle m \rangle}{\partial t} = \sum_{i=1}^{n}\sum_{j=1}^{n} -\frac{\partial a_i \langle m \rangle}{\partial x_i} + \frac{\partial^2 b_{ij}\langle m \rangle}{\partial x_i \partial x_j} - \gamma(x,t)\mathbb{P}(S_t = 1)p \tag{5.7}$$

And again replacing $p(\mathbf{x},t)\mathbb{P}(S_t = 1)$ by $\langle m \rangle$ gives as a result:

$$\frac{\partial \langle m \rangle}{\partial t} = \sum_{i=1}^{n}\sum_{j=1}^{n} -\frac{\partial a_i \langle m \rangle}{\partial x_i} + \frac{\partial^2 b_{ij}\langle m \rangle}{\partial x_i \partial x_j} - \gamma(x,t)\langle m \rangle \tag{5.8}$$

This equation can, just like the regular Kolmogorov forward equation, in a few steps be transformed into the form of an advection-diffusion equation. This is similar to what was done with the Kolmogorov forward equation.

In two dimensions the mass density is related to the concentration and water depth according to $\langle m(\mathbf{x},t)\rangle = c(\mathbf{x},t)H(\mathbf{x},t)$, making this substitution in two dimensions gives:

$$\frac{\partial Hc}{\partial t} = \sum_{i=1}^{2}\sum_{j=1}^{2} -\frac{\partial a_i Hc}{\partial x_i} + \frac{\partial^2 b_{ij} Hc}{\partial x_i \partial x_j} - \gamma(x,t)Hc \tag{5.9}$$

This is the same as:

$$\frac{\partial Hc}{\partial t} = \sum_{i=1}^{2}\sum_{j=1}^{2} -\frac{\partial a_i Hc}{\partial x_i} + \frac{\partial}{\partial x_i}\left(c\frac{\partial b_{ij}H}{\partial x_j} + b_{ij}H\frac{\partial c}{\partial x_j}\right) - \gamma(x,t)Hc \tag{5.10}$$

Rearrange the terms:

$$\frac{\partial Hc}{\partial t} = \sum_{i=1}^{2}\sum_{j=1}^{2} -\frac{\partial}{\partial x_i}\left(a_i Hc - \frac{\partial b_{ij}H}{\partial x_j}c\right) + \frac{\partial}{\partial x_i}\left(b_{ij}H\frac{\partial c}{\partial x_j}\right) - \gamma(x,t)Hc \tag{5.11}$$

Rewrite as:

$$\frac{\partial Hc}{\partial t} = \sum_{i=1}^{2}\sum_{j=1}^{2} -\frac{\partial}{\partial x_i}\left(a_i Hc - \frac{\partial b_{ij}}{\partial x_j}Hc - \frac{\partial H}{\partial x_j}b_{ij}c\right) + \frac{\partial}{\partial x_i}\left(b_{ij}H\frac{\partial c}{\partial x_j}\right) - \gamma(x,t)Hc \tag{5.12}$$

This equals:

$$\frac{\partial Hc}{\partial t} = \sum_{i=1}^{2}\sum_{j=1}^{2} -\frac{\partial}{\partial x_i}\left(\left(a_i - \frac{\partial b_{ij}}{\partial x_j} - \frac{b_{ij}}{H}\frac{\partial H}{\partial x_j}\right)Hc\right) + \frac{\partial}{\partial x_i}\left(b_{ij}H\frac{\partial c}{\partial x_j}\right) - \gamma(x,t)Hc \tag{5.13}$$

Filling in $b_{ij} = k_{ij}$ and $u_i = a_i - \frac{\partial b_{ij}}{\partial x_j} - \frac{b_{ij}}{H}\frac{\partial H}{\partial x_j}$, will result in the advection-diffusion equation with one extra term:

$$\frac{\partial Hc}{\partial t} = \sum_{i=1}^{2}\sum_{j=1}^{2} -\frac{\partial u_i Hc}{\partial x_i} + \frac{\partial}{\partial x_i}\left(k_{ij}H\frac{\partial c}{\partial x_j}\right) - \gamma(x,t)Hc \tag{5.14}$$

5.1.2. Method 2

This method is based on van den Boogaard et al. [17]. Now a new equation is defined that describes the time evolution of the particle's mass $M(t)$ as a SDE. The mass $M(t)$ is decreasing with fraction $\gamma(x,y,t)$ of the mass with each timestep. Adding this equation to the system of SDEs (equation 4.8), gives a new system of three SDEs:

$$\begin{aligned} dX(t) &= a_x(t)\cdot dt + \sigma(X,t)dW(t) \\ dY(t) &= a_y(t)\cdot dt + \sigma(Y,t)dW(t) \\ dM(t) &= -\gamma(x,y,t)\cdot M(t)\cdot dt \end{aligned} \tag{5.15}$$

A new probability density function is defined that is not only depending on the position but also the mass.

$$\hat{p}(t,x,y,m) = \lim_{\Delta x \downarrow 0, \Delta y \downarrow 0, \Delta m \downarrow 0} \frac{\mathbb{P}(x \le X(t) < x + \Delta x \wedge y \le Y(t) < y + \Delta y \wedge m \le M(t) < m + \Delta m)}{\Delta x \cdot \Delta m} \tag{5.16}$$

It can be shown that this equation satisfies the Fokker-Planck equation:

$$\frac{\partial \hat{p}}{\partial t} = -\sum_{i=1}^{2}\frac{\partial a_i \hat{p}}{\partial x_i} + \sum_{i=1}^{2}\sum_{j=1}^{2}\frac{\partial^2 b_{ij}\hat{p}}{\partial x_i \partial x_j} + \frac{\partial \gamma(t,x)m\hat{p}}{\partial m} \tag{5.17}$$

Now a mass density can be defined as the expected mass for particles at position (x, y) and time t:

$$\langle m(x,y,t)\rangle = \mathbb{E}(M(t)|X=x, Y=y) = \int m\hat{p}(x,y,t)dm \tag{5.18}$$

Each side of equation 5.17 is multiplied with m and integrated over m:

$$\int m\frac{\partial \hat{p}}{\partial t}dm = \int m\left(-\sum_{i=1}^{2}\frac{\partial a_i\hat{p}}{\partial x_i} + \sum_{i=1}^{2}\sum_{j=1}^{2}\frac{\partial^2 b_{ij}\hat{p}}{\partial x_i\partial x_j} + \frac{\partial\gamma(t,x)m\hat{p}}{\partial m}\right)dm \tag{5.19}$$

This can be rewritten as:

$$\int m\frac{\partial \hat{p}}{\partial t}dm = -\int m\left(\sum_{i=1}^{2}\frac{\partial a_i\hat{p}}{\partial x_i}\right)dm + \int m\left(\sum_{i=1}^{2}\sum_{j=1}^{2}\frac{\partial^2 b_{ij}\hat{p}}{\partial x_i\partial x_j}\right)dm + \int m\left(\frac{\partial\gamma(t,x)m\hat{p}}{\partial m}\right)dm \tag{5.20}$$

Now the derivation and summation operators can be placed outside the integral:

$$\frac{\partial}{\partial t}\int m\hat{p}dm = -\sum_{i=1}^{2}\frac{\partial}{\partial x_i}\int ma_i\hat{p}dm + \sum_{i=1}^{2}\sum_{j=1}^{2}\frac{\partial^2}{\partial x_i\partial x_j}\int mb_{ij}\hat{p}dm + \int m\left(\frac{\partial\gamma(t,x)m\hat{p}}{\partial m}\right)dm \tag{5.21}$$

Using the definition of $\langle m\rangle$ and partial integration on the last term, results into:

$$\frac{\partial}{\partial t}\langle m\rangle = -\sum_{i=1}^{2}\frac{\partial a_i\langle m\rangle}{\partial x_i} + \sum_{i=1}^{2}\sum_{j=1}^{2}\frac{\partial^2 b_{ij}\langle m\rangle}{\partial x_i\partial x_j} - \gamma(t,x)\langle m\rangle \tag{5.22}$$

This is the same result as equation 5.8 in method 1, therefore it can also be rewritten to the same advection-diffusion equation:

$$\frac{\partial Hc}{\partial t} = \sum_{i=1}^{2}\sum_{j=1}^{2} -\frac{\partial u_i Hc}{\partial x_i} + \frac{\partial}{\partial x_i}\left(k_{ij}H\frac{\partial c}{\partial x_j}\right) - \gamma(x,t)Hc \tag{5.23}$$

5.2. Lagrangian approach for the advection-diffusion equation with settling

In the previous section, the settling of particles was added to the advection-diffusion equation. Now this equation can also be solved in a similar way as the advection-diffusion equation was solved in chapter 4. The final result of method 1 and 2 was the same. Method 2 derived this result from the equations 5.15, this is already a system of Îto SDEs. Thus the Euler scheme can be used on these equations to gain the following numerical approximation:

$$\begin{aligned} X(t+\triangle t) &= X(t) + a_x(t)\triangle t + \sigma(X,t)(W_x(t+\triangle t) - W_x(t)) \\ Y(t+\triangle t) &= Y(t) + a_y(t)\triangle t + \sigma(Y,t)(W_y(t+\triangle t) - W_y(t)) \\ M(t+\triangle t) &= M(t) - \gamma M(t)\triangle t \\ X(0) = x_0, Y(0) &= y_0, M(0) = m_0 \end{aligned} \tag{5.24}$$

Again after simulating for a large number of particles a risk map could be made. Now the mass is also relevant for the probability to find a particle at a certain position. If the mass of the particles at that certain position is high, the chance to find a particle there is higher since this means that less particles settle while being transported to that position.

5.3. Settling of particles in the backward equation

The advection-diffusion equation that includes the settling can be used to add the settling of particles to the reverse time advection-diffusion equation. First, the backward equation for the settling term, $\frac{\partial\gamma(t,x)m(\cdot)}{\partial m}$, needs to be calculated. This will be done in the same way as shown for the Kolmogorov equation in the previous chapter, by finding the adjoint equation.

The definition of the adjoint (equation 3.17) is used again, filling in $\frac{\partial\gamma(t,x)m(\cdot)}{\partial m}$ gives:

$$\int_{-\infty}^{\infty} f(t,x,m)\frac{\partial\gamma(t,x)mg(t,x,m)}{\partial m}dm = \int_{-\infty}^{\infty} f(t,x,m)\left(\gamma(x,t)m\frac{\partial g(t,x,m)}{\partial m} + g(t,x,m)\frac{\partial\gamma(t,x)m}{\partial m}\right)dm \tag{5.25}$$

Which is the same as:

$$\int_{-\infty}^{\infty} f(t,x,m)\frac{\partial\gamma(t,x)mg(t,x,m)}{\partial m}dm = \int_{-\infty}^{\infty} f(t,x,m)\gamma(x,t)m\frac{\partial g(t,x,m)}{\partial m}dm + \int_{-\infty}^{\infty} f(t,x,m)g(t,x,m)\frac{\partial\gamma(t,x)m}{\partial m}dm \tag{5.26}$$

The derivative in the second integral is easy to calculate, so the equation can be rewritten as:

$$\int_{-\infty}^{\infty} f(t,x,m)\frac{\partial\gamma(t,x)mg(t,x,m)}{\partial m}dm = \int_{-\infty}^{\infty} f(t,x,m)\gamma(x,t)m\frac{\partial g(t,x,m)}{\partial m}dm + \int_{-\infty}^{\infty} f(t,x,m)g(t,x,m)\gamma(t,x)dm \tag{5.27}$$

Now take a look at the first integral of the right lid. Using partial integration the following equality is obtained:

$$\int_{-\infty}^{\infty} f(t,x,m)\gamma(x,t)m\frac{\partial g(t,x,m)}{\partial m}dm = \left[f(t,x)\gamma(x,t)mg(t,x,m)\right]_{-\infty}^{\infty} - \int_{-\infty}^{\infty}\frac{\partial f(t,x,m)\gamma(x,t)m}{\partial m}g(t,x,m)dm \tag{5.28}$$

The density functions are 0 at $\pm\infty$, so only the new integral needs to be taken into account. That integral can be written as:

$$\int_{-\infty}^{\infty}\frac{\partial f(t,x,m)\gamma(x,t)m}{\partial m}g(t,x,m)dm = \int_{-\infty}^{\infty}\left(\gamma(x,t)m\frac{\partial f(t,x,m)}{\partial m} + f(t,x,m)\frac{\partial\gamma(x,t)m}{\partial m}\right)g(t,x,m)dm \tag{5.29}$$

Which is the same as:

$$\int_{-\infty}^{\infty}\frac{\partial f(t,x,m)\gamma(x,t)m}{\partial m}g(t,x,m)dm = \int_{-\infty}^{\infty} g(t,x,m)\gamma(x,t)m\frac{\partial f(t,x,m)}{\partial m}dm + \int_{-\infty}^{\infty} g(t,x,m)f(t,x,m)\gamma(x,t)dm \tag{5.30}$$

This means that the total equation can be rewritten as:

$$\begin{aligned}\int_{-\infty}^{\infty} f(t,x,m)\frac{\partial\gamma(t,x)mg(t,x,m)}{\partial m}dm = &-\int_{-\infty}^{\infty} g(t,x,m)\gamma(x,t)m\frac{\partial f(t,x,m)}{\partial m}dm - \int_{-\infty}^{\infty} g(t,x,m)f(t,x,m)\gamma(x,t))dm \\ &+\int_{-\infty}^{\infty} f(t,x,m)g(t,x,m)\gamma(t,x)dm\end{aligned} \tag{5.31}$$

And that results in:

$$\int_{-\infty}^{\infty} f(t,x,m)\frac{\partial\gamma(t,x)mg(t,x,m)}{\partial m}dm = -\int_{-\infty}^{\infty} g(t,x,m)\gamma(x,t)m\frac{\partial f(t,x,m)}{\partial m}dm \tag{5.32}$$

Which means that $-\gamma(t,x)m\frac{\partial(\cdot)}{\partial m}$ is the adjoint of the operator $\frac{\partial\gamma(t,x)m(\cdot)}{\partial m}$.

5.4. Lagrangian approach for reverse time advection-diffusion equation with settling

In the previous chapter, the Kolmogorov backward equation had to be transformed into the same form as the Kolmogorov forward equation to be solved by the Lagrangian 'random walk' method. For the settling term the same kind of transformation is necessary:

$$-\gamma(t,x)m\frac{\partial(\cdot)}{\partial m} = -\frac{\partial\gamma(t,x)m(\cdot)}{\partial m} + (\cdot)\frac{\partial\gamma(t,x)m}{\partial m} \tag{5.33}$$

This is the same as:

$$-\gamma(t,x)m\frac{\partial(\cdot)}{\partial m} = -\frac{\partial\gamma(t,x)m(\cdot)}{\partial m} + (\cdot)\gamma(t,x) \tag{5.34}$$

Now these terms can be added to the Kolmogorov backward equation. This gives the following reverse time equation for two dimensions as a final result:

$$\frac{\partial\tilde{p}}{\partial s} = \sum_{i=1}^{2}\sum_{j=1}^{2}\frac{\partial\tilde{a}_i\tilde{p}}{\partial y_i} - \frac{\partial^2 b_{ij}\tilde{p}}{\partial y_i\partial y_j} + \tilde{p}\frac{\partial^2 b_{ij}}{\partial y_i\partial y_j} - \frac{\partial\gamma m\tilde{p}}{\partial m} + \gamma\tilde{p} \tag{5.35}$$

Or in the form of the reverse time advection-diffusion equation:

$$\frac{\partial H\tilde{c}}{\partial s} = \sum_{i=1}^{2}\sum_{j=1}^{2}\frac{\partial \tilde{u}_i H\tilde{c}}{\partial y_i} - \frac{\partial}{\partial y_i}\left(k_{ij}\frac{\partial H\tilde{c}}{\partial y_j}\right) + H\tilde{c}\frac{\partial^2 k_{ij}}{\partial y_i \partial y_j} - \frac{\partial \gamma m H\tilde{c}}{\partial m} + \gamma H\tilde{c} \tag{5.36}$$

The reverse time equation had some extra terms compared to the forward equation, so an extra weighing function was necessary to solve the reverse time advection-diffusion equation. In the backward equation that includes the settling, there are still extra terms present and the adjoint of the settling term even added more. Therefore again a weighing function is needed to solve this equation. The following system of SDEs is a solution for the reverse time advection-diffusion equation that includes the settling:

$$\begin{aligned} dX(s) &= \tilde{a}_x(s)\cdot ds + \sigma(X,s)dW_x(s) \\ dY(s) &= \tilde{a}_y(s)\cdot ds + \sigma(Y,s)dW_y(s) \\ dM(X,Y,s) &= \gamma(X,Y,s)M(X,Y,s)ds \\ d\mathcal{Z} &= \left(\frac{\partial^2 b_{xx}}{\partial x^2} + \frac{\partial^2 b_{xy}}{\partial x \partial y} + \frac{\partial^2 b_{yy}}{\partial y^2} + \frac{\partial^2 b_{yx}}{\partial y \partial x} + \gamma(s,y)\right)\mathcal{Z}\,ds \end{aligned} \tag{5.37}$$

Similarly to the previous systems of SDEs, this can be solved with the Euler scheme.

$$\begin{aligned} X(s+\triangle s) &= X(s) + \tilde{a}_x(s)\triangle s + \sigma(X,s)(W_x(s+\triangle s) - W_x(s)) \\ Y(s+\triangle s) &= Y(s) + \tilde{a}_y(s)\triangle s + \sigma(Y,s)(W_y(s+\triangle s) - W_y(s)) \\ M(X,Y,s+\triangle s) &= M(X,Y,s) + \gamma(X,Y,s)M(X,Y,s)\triangle s \\ \mathcal{Z}(s+\triangle s) &= \mathcal{Z}(s) + \left(\frac{\partial^2 b_{xx}}{\partial x^2} + \frac{\partial^2 b_{xy}}{\partial x \partial y} + \frac{\partial^2 b_{yy}}{\partial y^2} + \frac{\partial^2 b_{yx}}{\partial y \partial x} + \gamma(s,y)\right)\mathcal{Z}(s)\triangle s \\ X(0) = x_0, Y(0) &= y_0, M(0) = m_0, \mathcal{Z}(0) = 1 \end{aligned} \tag{5.38}$$

In the previous chapter was explained that in the simulations of this project, b_{ij} is defined constant. This means that $\mathcal{Z}$ can be simplified to:

$$\mathcal{Z}(s+\triangle s) = \mathcal{Z}(s) + \gamma(s,y)\mathcal{Z}(s)\triangle s$$

Again after simulating for a large number of particles, a risk map can be made. When a risk map is made of these results, the position, mass and weight of the particles need to be taken into account. When a particle has a higher mass and weight, that means that the chance that this position is the source of the particle is higher. By multiplying the mass and the weight of a particle, its 'weighted mass' is obtained. This weighted mass can be used to make a risk map to indicate which positions have a higher chance to be the origin of a particle.

5.5. Settling probabilities

The settling of particles is now added to the advection-diffusion equation but the value for γ still needs to be derived. This is done by comparing simulations using the settling rate γ with simulations using the settling probabilities that are used when settling is not incorporated into the advection-diffusion equation.

5.5.1. Settling probability for macroplastics

The macroplastics considered in this model are floating. The probability to settle is depending on the kind of plastic (i.e. size, density, shape) and the water properties (i.e. salinity and temperature). Also the weather conditions are of importance, they can change the speed of degradation or biofouling (a layer of micro-organisms accumulating on the surface). Up to this moment, only little research is done on the settling probability of macroplastics. In these simulations a settling time, τ_{settle}, of 10 days is chosen (Critchell and Lambrechts [4]). This means that each time step the macroplastics have the following probability to settle:

$$\mathbb{P}_{macro}^{settle} = \frac{\Delta t}{\tau_{settle}} \tag{5.39}$$

5.5.2. Settling probability for microplastics

The microplastics are assumed to be homogeneously spread through the water column but they also have a chance to sink to the sea floor. Due to this spreading through the water column, the probability to settle is smaller when the water is deeper. For microplastics a sinking velocity, w_{settle} is used. This is again largely

depending on for example size, density and shape of the plastic, but also the salinity and temperature of the water (Kowalski et al. [11]). In these simulations a value of $5 \cdot 10^{-5}$ was chosen for w_{settle} (Critchell et al. [5]). Each time step the microplastics have the following chance to settle:

$$\mathbb{P}_{micro}^{settle} = \frac{w_{settle}\Delta t}{H(x,y,t)} \tag{5.40}$$

5.5.3. Settling rate for macro- and microplastics

In the previous two sections, probabilities for settling are defined. However, these need to be transformed into suitable values for γ, which will be called the settling rate.

The value of γ was found by doing the simulations of the settling of plastic particles twice. First by simulating for 1000 particles that each time step they had the chance to settle as defined above. Next by assigning a mass of 10 g for the macroplastics and 10 mg for the microplastics to each of the 1000 particles. Each time step that mass would decrease by γ multiplied with the mass of the particle in the previous time step. γ was changed till the ratios of settled mass and initial mass of the two methods were approaching each other. For microplastics, the found settling rate was $4 \cdot 10^{-5}$ and for macroplastics that value was $11 \cdot 10^{-5}$.

6

Simulations

This chapter will first explain the test case used to simulate the movement and settling of plastic particles. This is followed by an explanation and the results of some simplified simulations. These simulations were done to validate the chosen number of particles and time step and to show the necessity of the correction velocity described in section 4.4. Next the results of the simulations will be shown using several figures generated with MATLAB.

6.1. Test case

The test case that will be used for the simulations is quite a simplified situation compared to reality. The area that is simulated can be seen as an extremely large pool of water (large enough that the particles do not move against or across the borders) with a linearly increasing water depth in the positive y-direction. At point (x,0) the water is 25m deep and its depth increases with 0.2 millimetre per metre in the positive y-direction. The starting position of the particles in the simulations was $(x, y) = (0, 0)$.

The simulations were done for 1000 particles. The timespan of the simulations was 14 days and the time step was 900 seconds. The initial mass of the particles was 10 g for the macroplastics and 10 mg for the microplastics.

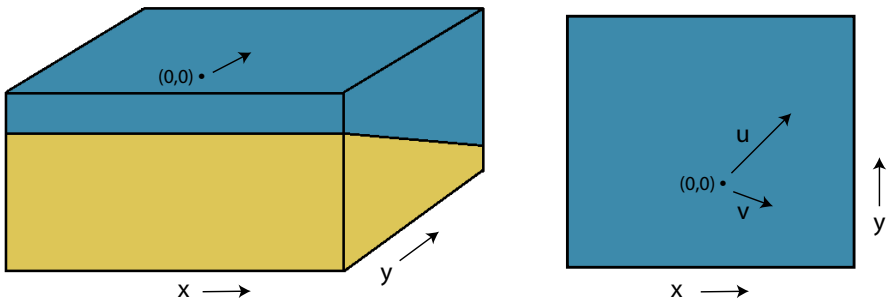

Figure 6.1: The situation that is simulated is shown in these images. The image on the left shows that the simulated area can be seen as an extremely large pool with a linearly increasing water depth. The image on the right gives a schematic view from above, including the vectors for the water velocity (u) and wind velocity (v).

A lot of parameters are affecting the behaviour of plastic particles. In these simulations some of the parameters are defined constant even though it is more realistic that they would vary in time and/or space. This is the simulation of a general situation instead of a specific coastal area and period in time, so it would not increase the insights gained by these simulations to vary all parameters in time and/or space. This was already discussed briefly for the diffusivity and settling probabilities. Other parameters that are consciously defined constant, are the wind and water velocity (u and v). It was quite hard to find data for these velocities and again varying them in time and space would not give more insight in the model. The wind and water

velocity were chosen in an arbitrary direction and with a plausible magnitude. Table 6.1 gives an overview of the values for different constants used in the model.

time step	Δt	900	$[s]$
diffusivity	κ	10	$[m^2/s]$
water velocity in x-direction	u_x	0.5	$[m/s]$
water velocity in y-direction	u_y	0.5	$[m/s]$
wind velocity in x-direction	v_x	1.5	$[m/s]$
wind velocity in y-direction	v_y	-0.5	$[m/s]$
wind drift coefficient	α	0.03	[-]
settling time for macroplastics	τ_{settle}	10	[days]
settling velocity for microplastics	w_{settle}	$5 \cdot 10^{-5}$	$[m/s]$
settling rate for macroplastics	γ_{macro}	$11 \cdot 10^{-5}$	[-]
settling rate for microplastics	γ_{micro}	$4.0 \cdot 10^{-5}$	[-]

Table 6.1: Constants used in the simulations.

For the reverse time simulations the same constants were used. Again the starting position was $(x, y) = (0, 0)$. In these simulations the water depth was at that point defined as 130m and the depth decreased with 0.2 millimetre per metre in the negative y-direction. For the reverse time simulations the initial mass for macroplastics was 3 g and for microplastics 6.5 mg. These were approximately the masses of the particles at the end of the forward simulations.

6.2. Numerical validation

The numerical error in the simulations is caused by the number of particles and time step. The number of particles needs to be sufficiently large and the time step sufficiently small to obtain useful results. However, simulating for too many particles and/or time steps can make the computations extremely time consuming. To check if these parameters are chosen adequate, some simplified simulations are done. If the number of particles and time step are fine for these simulations, they should also be sufficient for the more complicated simulations.

First, some one dimensional simulations for microplastics were done without settling and with a constant water depth and diffusivity. This means that the movement of the particles was due to current and dispersion. The analytical solution for this one dimensional situation is equal to:

$$p(x, t) = \frac{1}{\sqrt{2\kappa t}} \exp^{-\frac{x-ut}{2\kappa t}} \tag{6.1}$$

with u the constant water velocity, κ the constant diffusivity. This is a moving and broadening Gaussian distribution. (Brics et al. [1])

Simulations were done for 250, 500, 1000 and 2000 particles and with a time step of 450, 900, 1800 and 3600 seconds. The particles started at $x = 0$ and the timespan was 14 days. The results were plotted as histograms. To compare the histograms with the correct distribution, the analytical solution was scaled for the different numbers of particles and plotted in the same figures. These graphs can be seen in the following figures.

In the previous section was already mentioned that a time step of 900 seconds and 1000 particles were chosen as parameters. Those values gave correct results for the simplified simulations and did not result in an extremely long computation time.

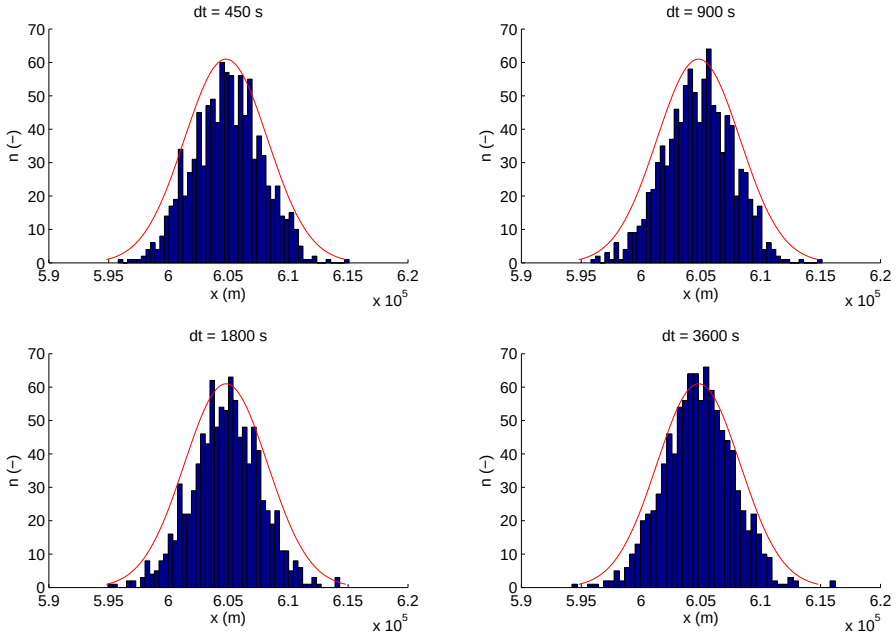

Figure 6.2: These four graphs show the histogram of the one dimensional simulations for four different time steps (450, 900, 1800 and 3600 seconds). The timespan was 14 days and these simulations were done with 1000 particles. The red line is the analytical solution for the same situation. A smaller time steps should produce better results but for this situation all time steps seem to be sufficiently small to generate a correct histogram.

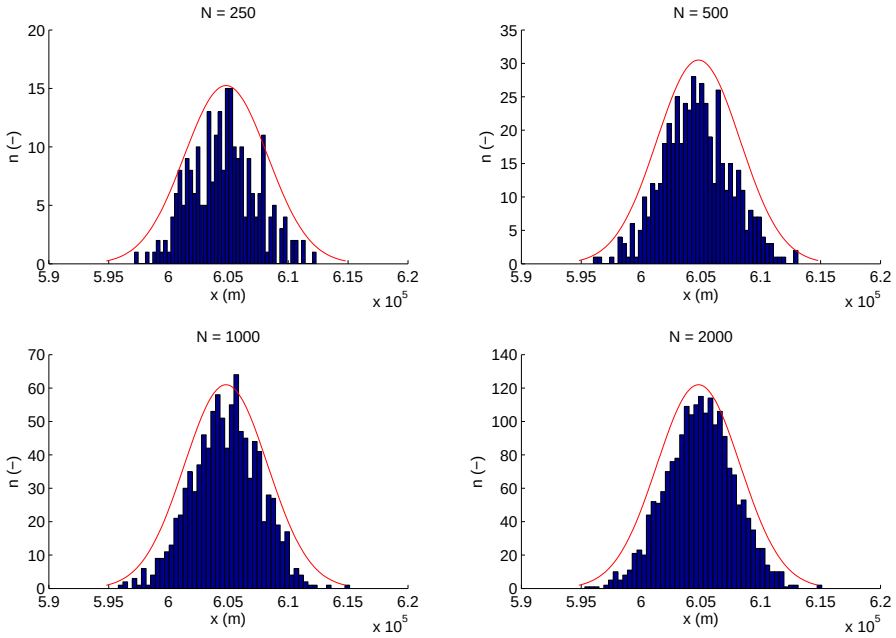

Figure 6.3: These four graphs show the histogram for the one dimensional simulations for four different numbers of particles (250, 500, 1000 and 2000 particles). The timespan was 14 days and the time step was 900 seconds. The red line shows the analytical solution for the same situation. As expected the results improve when the number of particles increases but all four histograms have a shape that is comparable to the analytical solution.

Next, some simplified simulations were done for a varying water depth and constant diffusivity. The purpose of these simulations was to show the necessity of adding the correction velocity discussed in section 4.4 to the drift term when the water depth is not constant.

Again the simulations were done for microplastics in a one dimensional situation without settling. For these simulations the current is omitted, so the particles are only moving due to dispersion. The starting position of the particles was $x = 5 \cdot 10^4$m and the timespan was again 14 days with a time step of 900 seconds.
The water depth is defined as a sine wave depending on x:

$$H(x) = 25 + 20 \sin\left(\frac{2\pi x}{10^5}\right)$$

This means the correction velocity is equal to:

$$\tilde{u} = \kappa \frac{40\pi \cos\left(\frac{2\pi x}{10^5}\right)}{10^5 H(x)}$$

A space varying water depth makes the advection-diffusion equation more complex, so it is harder to determine the analytical solution. Therefore a numerical solver was used to obtain a correct solution. The function pdepe() was used in MATLAB to solve the partial differential equation numerically. This function solves one dimensional initial-boundary value problems for systems of parabolic and elliptic partial differential equations. (MathWorks [12])

Simulations were done twice for 1000 particles, once with the correction velocity and once without. Again the results are represented in two separate histograms. The numerical solution was plotted in the same figures to compare the histograms with the correct distribution. The results for these simulations are shown in the next figures.

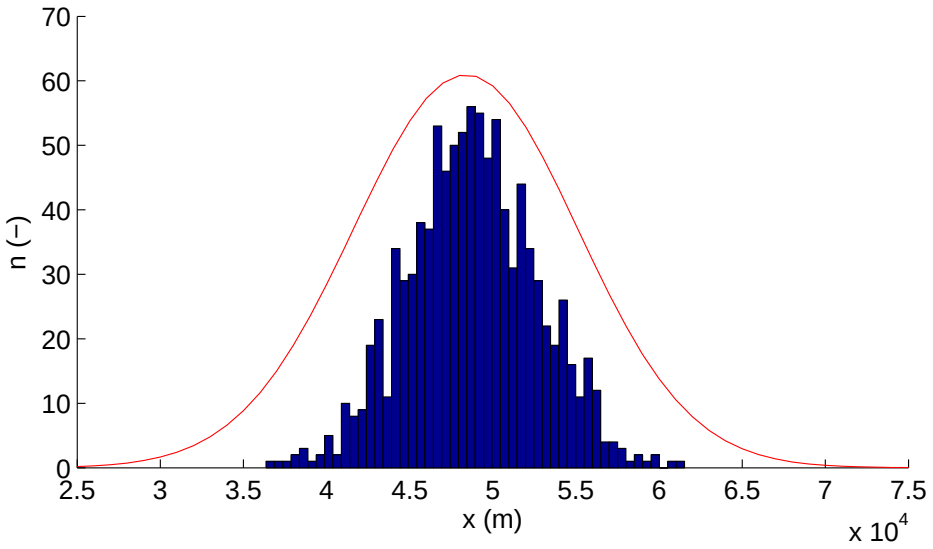

Figure 6.4: The histogram shows the results for the one dimensional simulations with the correction velocity. The red line is the numerical solution. The histogram is situated in the middle of the numerical solution as expected.

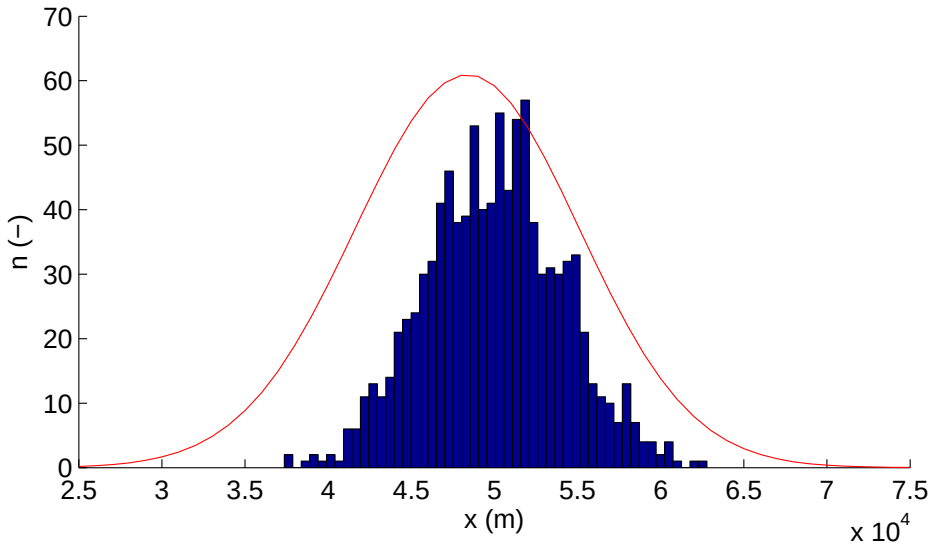

Figure 6.5: The histogram shows the results for the one dimensional simulations without the correction velocity. The red line is the numerical solution. The histogram is situated more to the right then the numerical solution, this is due to the lacking correction velocity.

The difference between the two figures is not enormous but these results do show that the correction velocity is a necessary addition to the drift term. Especially when the bathymetry is more complex and there is also a space varying diffusivity, the correction velocity as defined in section 4.4 should not be omitted.

6.3. Results

The following pages will show the outcomes of the implemented model, using some of the figures generated in MATLAB. First the results for the forward simulations of macroplastics and subsequently microplastics will be shown. Thereafter the results for the reverse time simulations will be shown for respectively the macro- and microplastics.

In Chapter 5 the advection-diffusion equation that included settling was obtained. To check if the simulations for this equation matched the method of settling probabilities, the forward simulations were done in two different ways: using the settling probabilities and the settling rates. This way the results for the obtained advection-diffusion equation with settling can be compared with the more common way of simulating by using settling probabilities. The backward simulations were only done using the method of settling rates.

As was already mentioned, the solution of the Kolmogorov equation can be used to make a risk map of the area where the particles can be found at a certain time. In this report the risk map is in the form of an histogram. The height of the bars is proportional to how high the risk is to find a particle at that position. In these simulations the peak is quite narrow, this is due to the extremely simple velocity field and a diffusivity that is not very high. In reality it can be expected that the plastic will spread out more.

6.3.1. Forward time simulations of macroplastics

The first figure is the histogram of the area where the unsettled macroplastics are positioned after the simulation of 14 days. This was done for the simulation using settling rates. As expected the particles are spread out due to the dispersion but there is a clear area where the particles will probably end up. In the centre of this area the peaks are roughly highest and towards the edges the peaks become lower. This is also the same as expected.

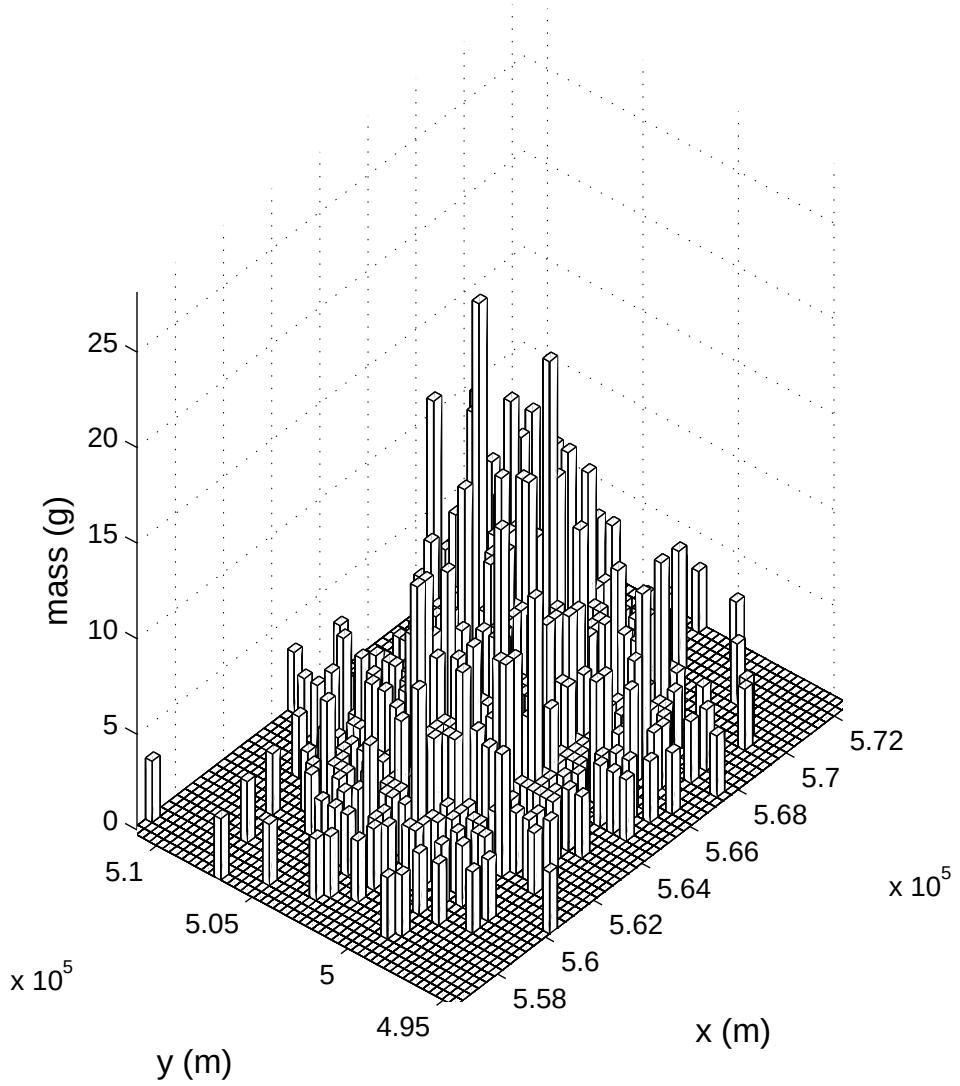

Figure 6.6: This figure is a histogram of the area where macroplastics were positioned after the simulation using the settling rates. The hight of the bars equals the sum of the mass of the particles in that bin. This means that a higher bar is equivalent to a higher probability to find a particle at that position. This figure makes clear that the highest probability to find a particle is in the centre of this area and this probability decreases at the positions further from the centre.

The next two figures show what path the particles followed. The starting point was (0,0) and the particles moved in the positive x- and y-direction. In the first figure the yellow line indicates the path that would be used if there was no dispersion, the blue lines are the paths taken with dispersion. It is clear that over time, due to dispersion the particles spread out more. In the second figure the decrease in mass is incorporated. The colour of the graph indicates the mass at that point. The figure shows that the mass of the particles decreases over time.

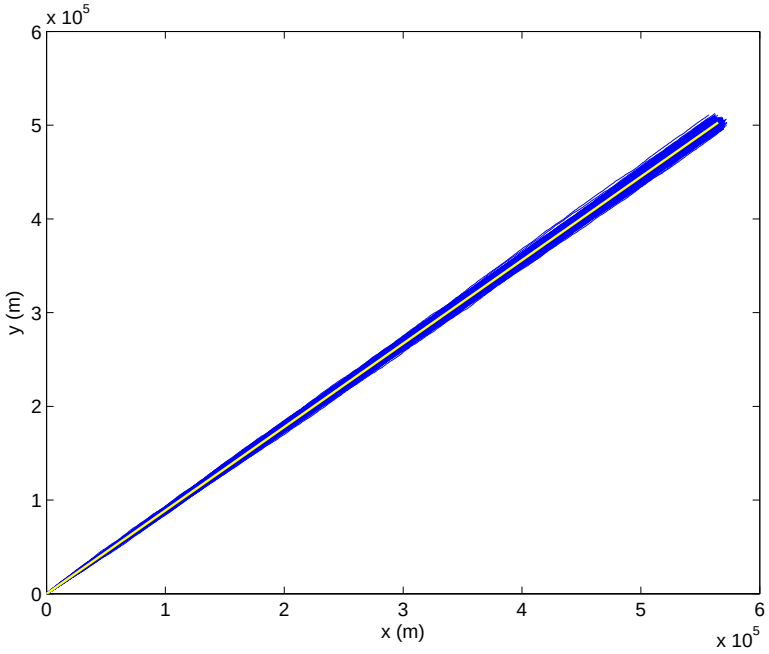

Figure 6.7: In this figure the paths of all macroplastics are plotted together. The starting point was (0,0) and the particles are moving in the positive x- and y-direction. The yellow line shows the path taken when there would be no dispersion. As the particles are moving further from their starting point the variation from the path without dispersion is increasing.

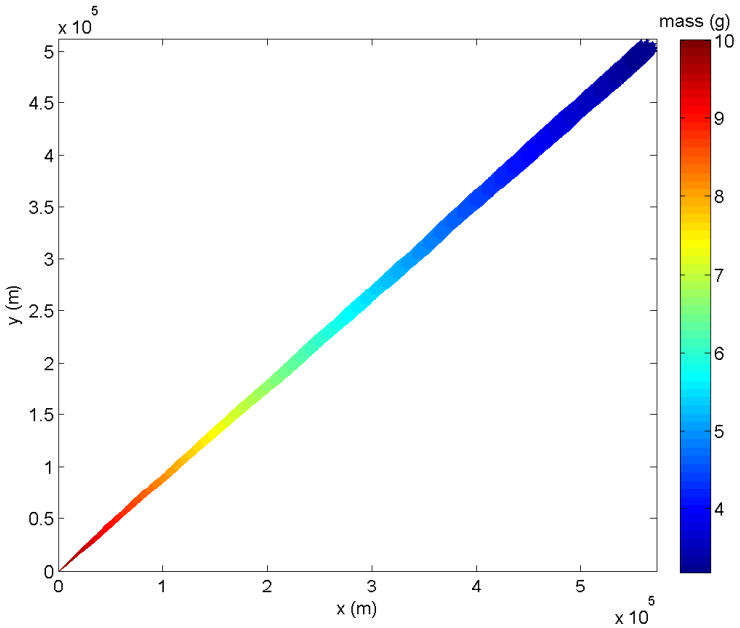

Figure 6.8: In this figure the paths and mass of all macroplastics are plotted. The starting point was (0,0) and the particles are moving in the positive x- and y-direction, the mass of the macroplastics was 10 g at the starting point. The colour of the graph indicates the mass of the particles. The mass is decreasing as the particles move further from their starting point because more of the mass has settled.

The following figures can be used to compare the two methods of modelling the settling of particles. The next two figures show the position of the particles at different times within the timespan of 14 days. The radius of the marker is an indicator for the mass of the macroplastics. The first figure shows the results for the simulations using the settling probability and the second figure is for the settling rate.

It is clear that the velocity and rate of spreading of the macroplastics were equal in both simulations. The clear difference between the two methods is the mass of the particles. In the first figure the mass is unchanged while in the second figure the mass has decreased. In the first figure the amount of particles has decreased over time but this is hardly visible.

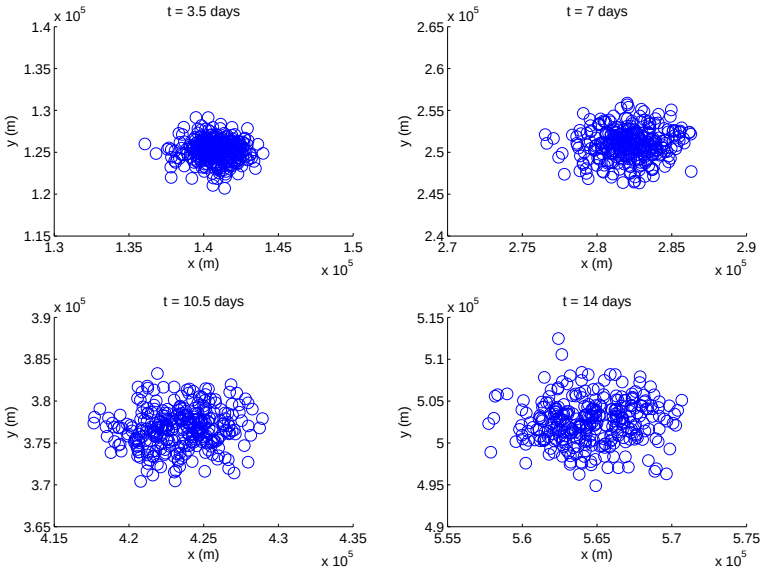

Figure 6.9: These figures show the macroplastics at 4 times modelled with the method using the settling probability. The mass of the particles (indicated by the radius of the markers) is not decreasing over time but the amount of particles does decrease. Over time the particles are moving in the positive x- and y-direction and the spreading of the particles is increasing.

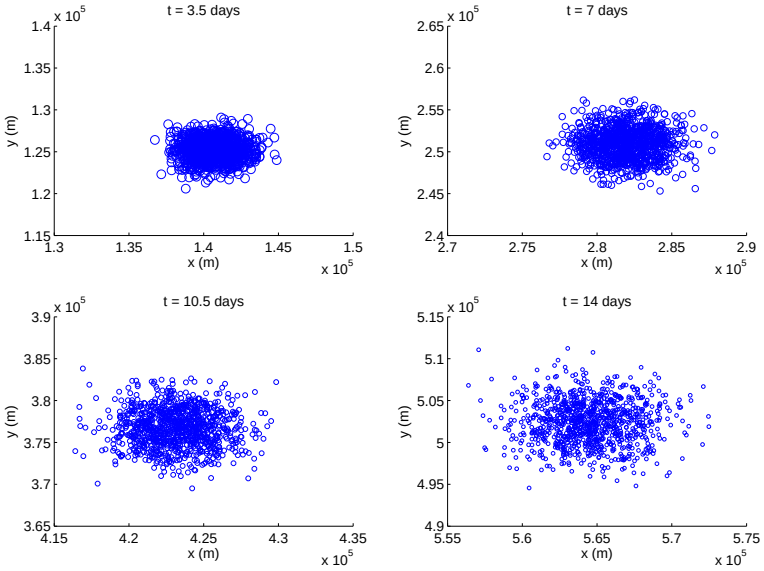

Figure 6.10: These figures show the macroplastics at 4 times modelled with the method using the settling rate. The mass of the particles (indicated by the radius of the markers) is decreasing over time and the amount of particles is unchanged. Over time the particles are moving in the positive x- and y-direction and the spreading of the particles is increasing.

To compare the decrease of mass in both simulations another figure was made. Now the fraction of the mass that had not settled is plotted over time. For the method using the settling rate this resulted in a smooth line while the method using the settling probability is less smooth. Overall the lines are very similar as was expected.

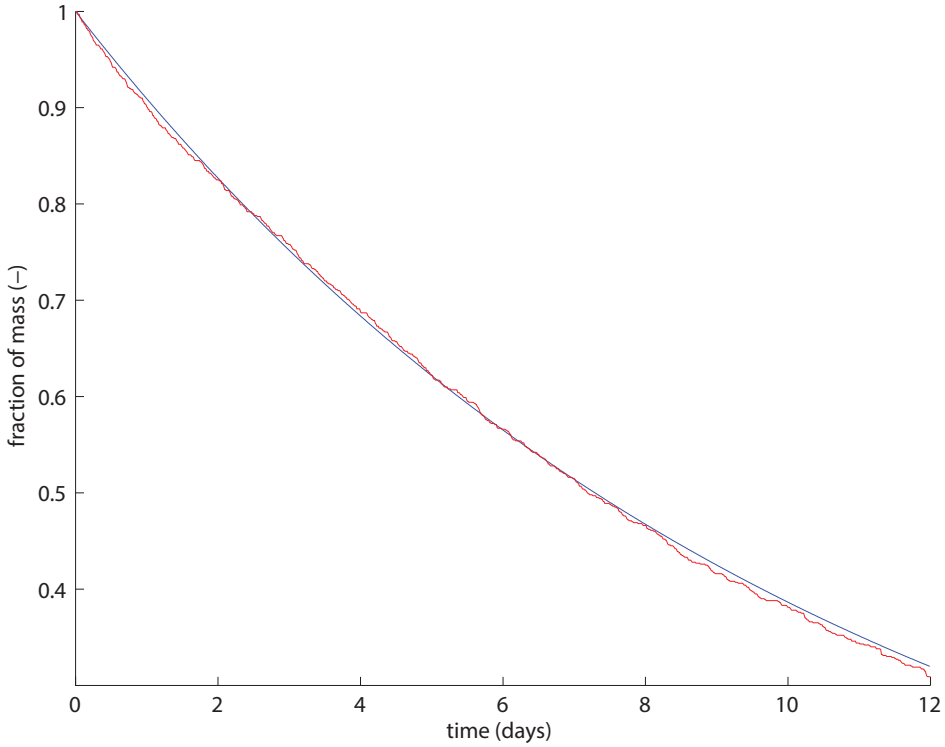

Figure 6.11: This figure shows the ratio between the mass of the macroplastics at each point in time and the original total mass. The red line shows this fraction for the simulation using the settling probability. The blue line shows the fraction for the simulation using the settling rate. The red line is less smooth than the blue line but overall the two lines have similar characteristics.

6.3.2. Forward-time simulations of microplastics

Now the figures for the forward simulation of microplastics will be shown. As expected most of the generated figures for microplastics are comparable to the figures for macroplastics from the previous section.

The first figure is again a histogram of the area where the unsettled particles are positioned at the end of the simulations. The height of the bar is the sum of the masses of the particles that are positioned there. This means that a high bar indicates a higher probability to find a particle at that position. The shape of the histogram can be compared with a cone, the bars in the middle are the highest and at the edges the bars become lower. This means that the probability to find a particle is highest in the centre of this area.

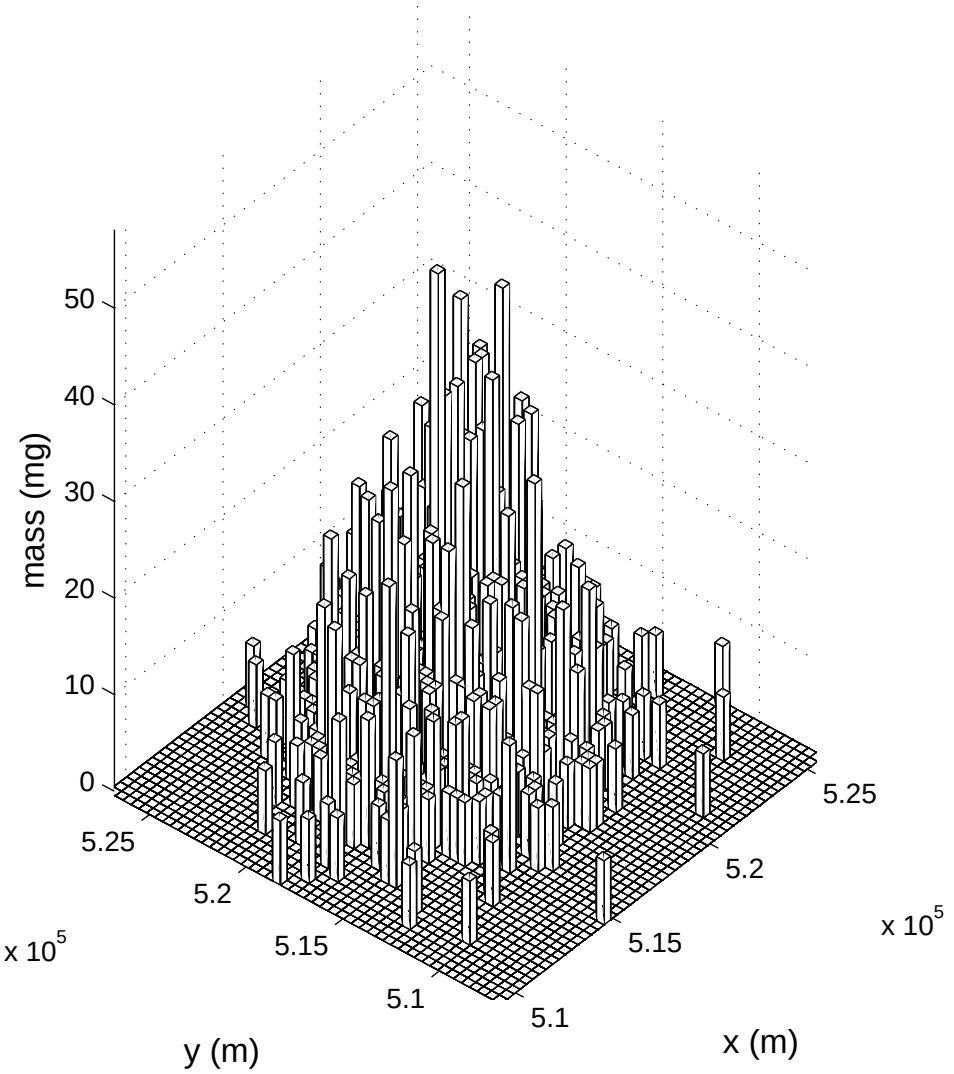

Figure 6.12: This is a histogram of the area where microplastics were positioned after the simulation. The hight of the bars equals the sum of the mass of the particles in that bin. This means that a higher bar is equivalent to a higher probability to find a particle at that position. Clearly the probabilities are highest in the centre of this area and lower at the edges.

The next two figures show what path the microplastics followed. The starting point was (0,0) and the particles moved in the positive x- and y-direction. In the first figure the light line indicates the path that would be used if there was no dispersion and the blue lines are the paths taken with dispersion. Clearly the the particles spread out more over time. In the second figure the decrease in mass is visible. The colour of the graph indicates the mass at that point. The figure shows that the the mass of the particles decreases as they move further from the source.

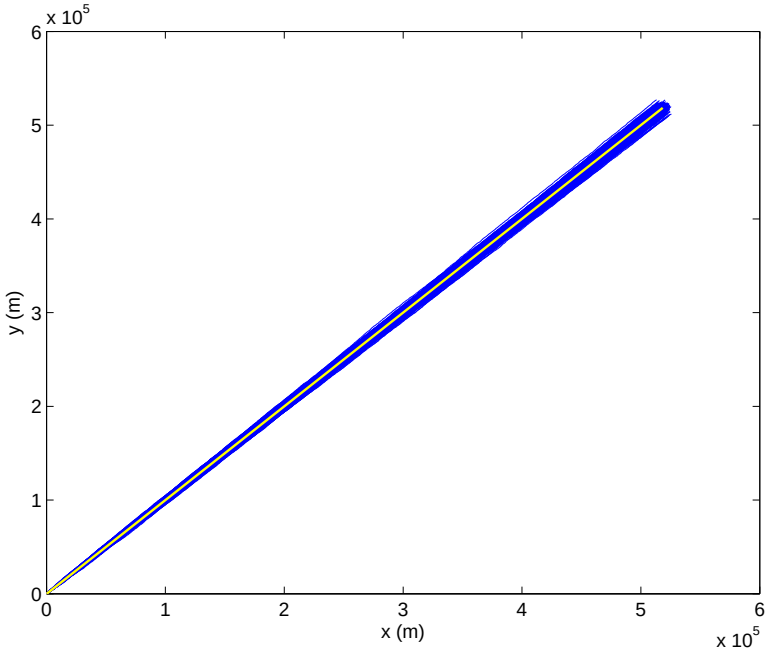

Figure 6.13: In this figure the paths of all the microplastics are plotted together. The starting point was (0,0) and the particles are moving in the positive x- and y-direction. The light line shows the path that would be taken if there was no dispersion. As the particles move further from their starting point the variation from the path without dispersion is increasing.

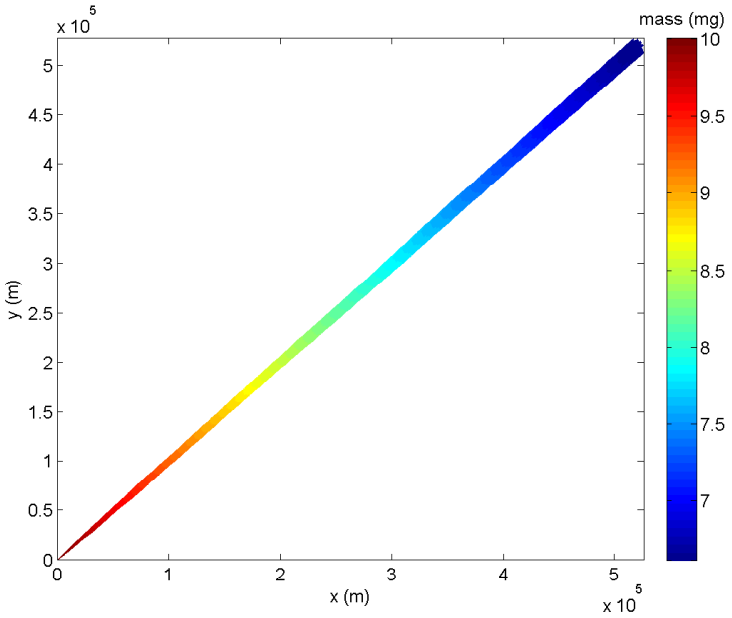

Figure 6.14: In this figure the paths and mass of all microplastics are plotted. The starting point was (0,0) and the particles are moving in the positive x- and y-direction, the mass of the microplastics was 10 mg at the starting point. The colour of the graph indicates the weight of the particles. Due to settling the mass of the particles is decreasing as they move further from their starting point.

The following figures can be used to compare the two methods of modelling the settling of particles. The next two figures show the position of the particles at different times within the timespan of 14 days. The radius of the marker is an indicator for the mass of the microplastics. The first figure shows the results for the simulations using the settling probability and the second figure for the settling rate.

These figures show that the velocity and rate of spreading of the microplastics were equal in both simulations. The clear difference between the two methods is the mass of the particles. In the first figure the mass is unchanged while in the second figure the mass has decreased. These figures also make clear that the mass of the microplastics is relatively less quickly decreasing than the mass of the macroplastics.

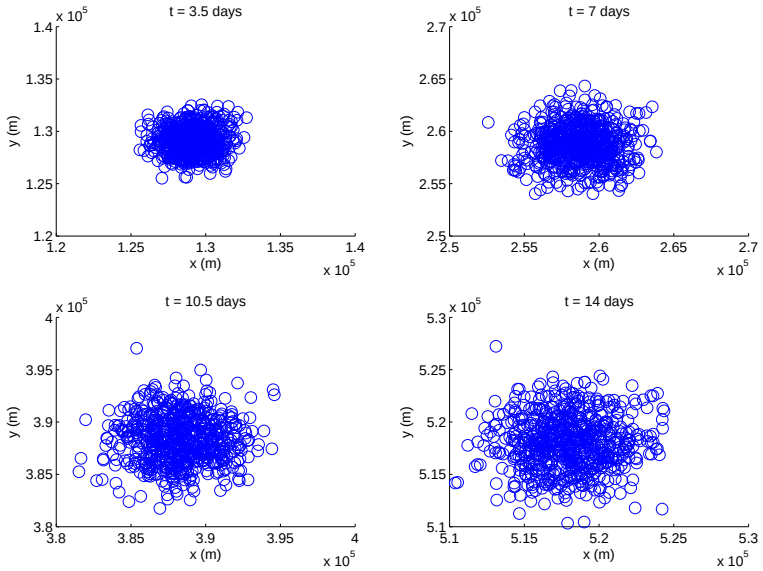

Figure 6.15: These figures show the microplastics at 4 times modelled with the method using the settling probability. The mass of the particles (indicated by the radius of the markers) is not decreasing over time. The amount of particles does decrease but not enough to be visible. Over time the particles are moving in the positive x- and y-direction and the spreading of the particles is increasing.

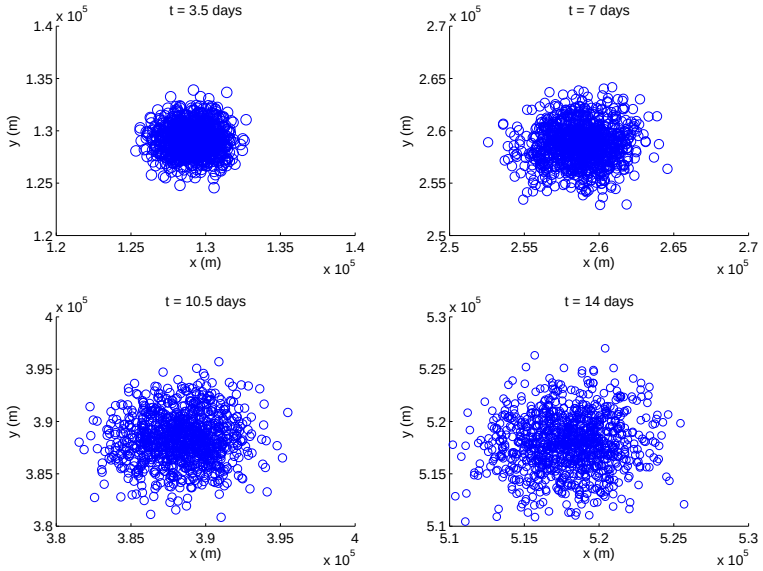

Figure 6.16: These figures show the microplastics at 4 times modelled with the method using settling rates. The mass of the particles (indicated by the radius of the markers) is decreasing over time and the amount of particles is unchanged. Over time the particles are moving in the positive x- and y-direction and the spreading of the particles is increasing.

To compare the decrease of mass in both simulations, again a figure was made that plots the fraction of the mass that had not settled over time. In contrast to the simulations for macroplastics, this did not result in similar lines for both methods right away. The two lines are further apart and the settling rate seems to result in a more linear line than using the settling probability. This difference could be explained by the fact that the settling probability for microplastics is depending on the water depth while the settling rate was defined constant. This was solved by finding new definition for γ, where γ was inversely proportional to the water depth: $\gamma = \frac{2.48 \cdot 10^{-5}}{H}$. The results for this settling rate can be seen in the second figure and are much better.

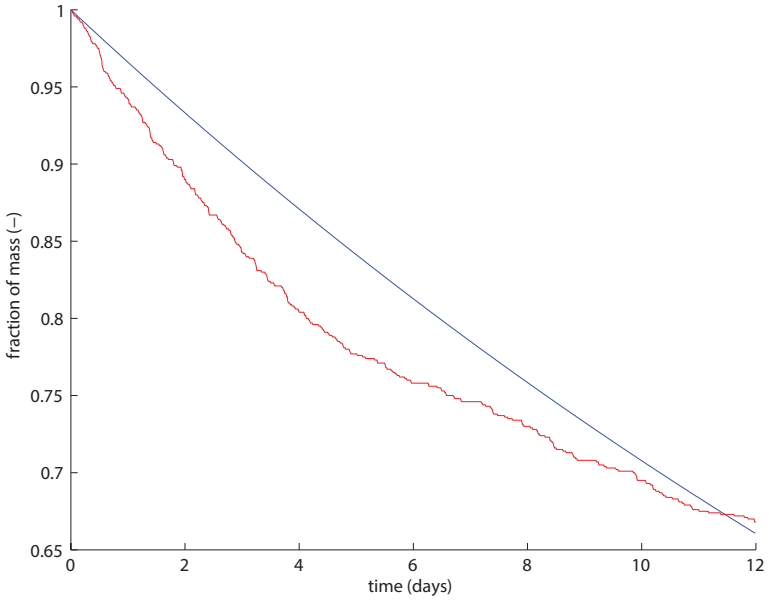

Figure 6.17: This figure shows over time the ratio between the total mass of the macroplastics and their original total mass. The red line shows this fraction for the simulations using the settling probability. The blue line shows the fraction for the simulations using the constant settling rate of $11 \cdot 10^{-5}$. The red line is not only less smooth than the blue line but also has a different curvature.

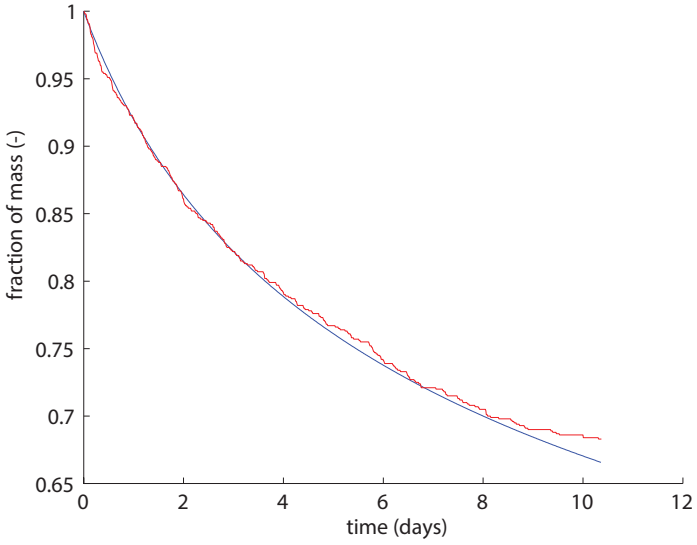

Figure 6.18: This figure shows over time the ratio between the total mass of the microplastics and their original total mass. The red line shows this fraction for the simulations using the settling probability.The blue line shows the fraction for the simulations using the settling rate of $\frac{2.48 \cdot 10^{-5}}{H}$. The red line is less smooth than the blue line but the two lines have similar characteristics.

The next figure shows the difference in path between the macro- and microplastics. Their general direction is the same, this is as expected since both kind of particles are mainly transported by the same current. However their exact direction is slightly different. Apart from the current, the macroplastics were also affected by the wind, which was directed in the positive x-direction and the negative y-direction. The microplastics were affected by the bathymetry gradient, which caused a movement in the positive y-direction due to the linearly decreasing water depth. These difference can be seen in this graph since the paths of the microplastics are slightly higher than the paths of the macroplastics. That means the y-coordinate of the microplastics is a little higher than that of the macroplastics.

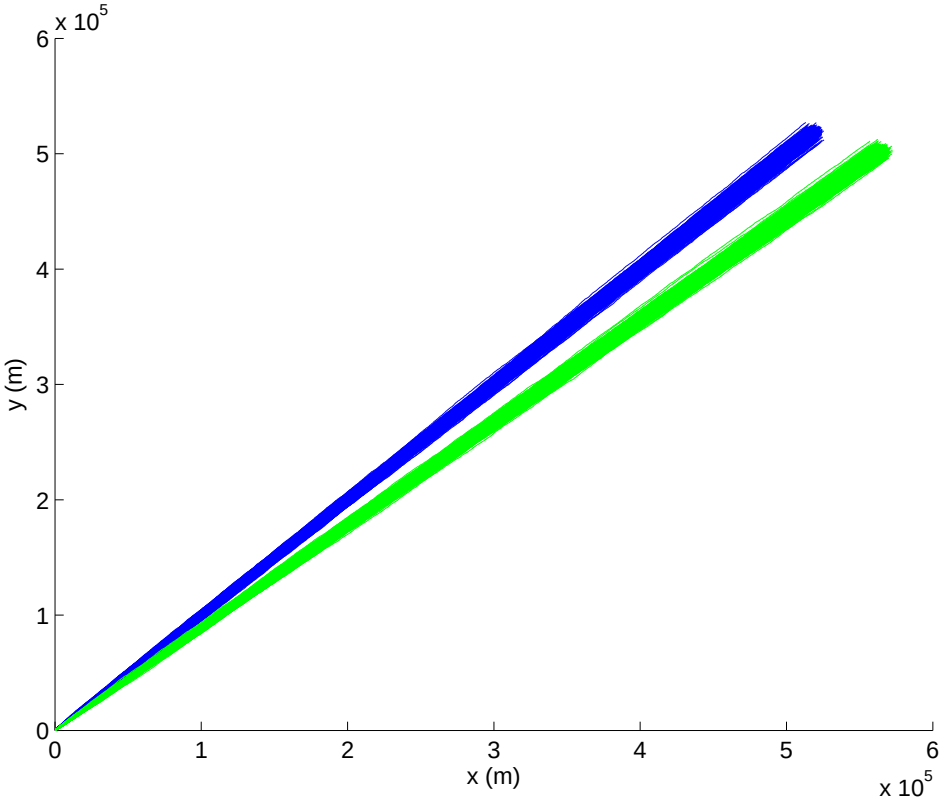

Figure 6.19: The paths of the macroplastics (green) and microplastics (blue) are plotted together in the same figure. Their general direction is similar, both are moving in the positive x- and y direction, but the exact direction is slightly different due to differences in their drift terms. As the particles are moving further from their starting point they are diverging more. The amount of spreading of the macro- and microplastics is comparable.

6.3.3. Reverse-time simulations for macroplastics

Now the results for the reverse time simulation of the macroplastics will be shown. These figures will have many similarities with the forward simulations but there are also differences that will be pointed out.

In this section, the first figure is again a histogram. The height of the bars is proportional to the probability that the particle found at (0,0) was released at that position. For the reverse time simulations, the bars are the sum of 'weighted mass' (the mass multiplied with the weight of the particle) of the particles in that bin. The shape of the histogram is similar to the previous ones with the highest bars in the centre of the area and lower bars at the edges.

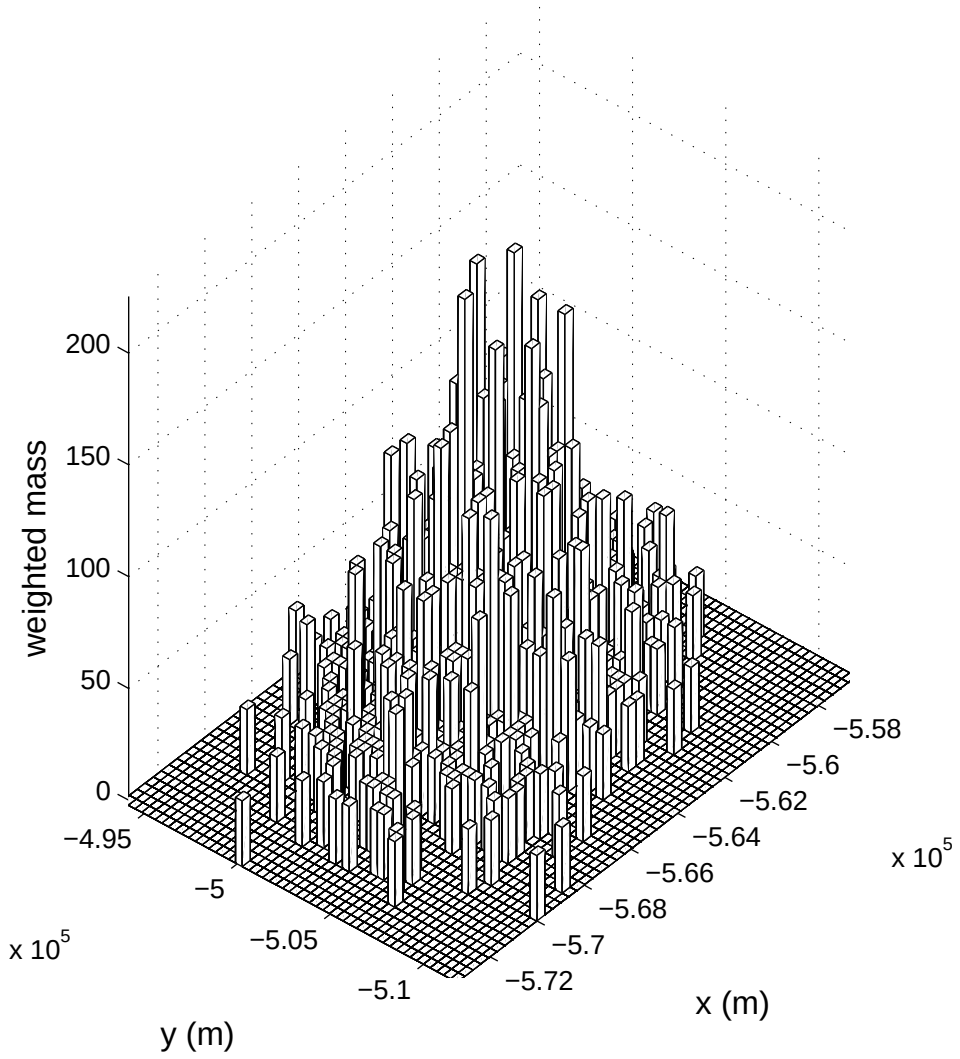

Figure 6.20: This figure is a histogram of the area where macroplastics were positioned after the reverse time simulation. The hight of a bar equals the sum of the 'weighted mass' of the particles in that bin. This means that a higher bar is equivalent to a higher probability a particle had its origin at that position.

The next two figures show what path the macroplastics followed in the reverse time simulations. The starting point was (0,0) and the particles moved in the negative x- and y-direction. In the first figure the light line indicates the path that would be used if there was no dispersion and the blue lines are the paths taken with dispersion. It is clear that over time the particles are spread out more due to dispersion. In the second figure the increase in mass is incorporated. The colour of the graph indicates the mass at that point. In these simulations the mass is increasing instead of decreasing over time. This makes sense since the process of settling is reversed in these simulations. As expected the position and mass of the particles is changing in the opposite direction compared to the forward simulations.

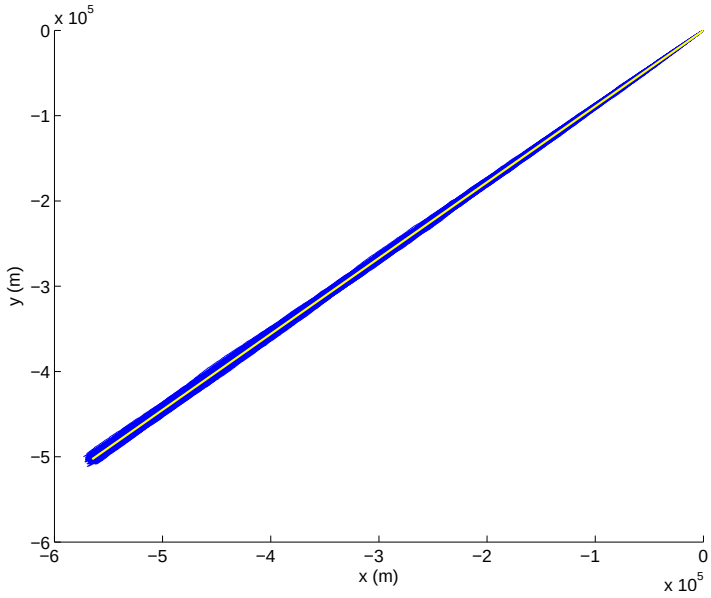

Figure 6.21: In this figure the reverse time paths of all the macroplastics are plotted together. The starting point was (0,0) and the particles are moving in the negative x- and y-direction. The light line shows the path taken when there would be no dispersion. As the particles are moving further from their starting point the variation from the path without dispersion is increasing.

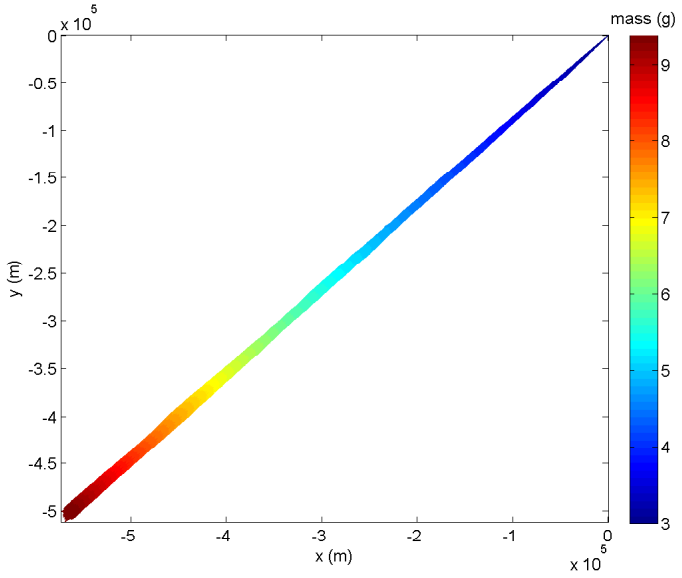

Figure 6.22: In this figure the reverse time paths and mass of all macroplastics are plotted. The starting point was (0,0) and the particles are moving in the negative x- and y-direction. The mass of the macroplastics was 3 g at the starting point. The colour of the graph indicates the weight of the particles. The mass is increasing as the particles move further from their starting point because the process of settling is also reversed.

In the next figure the positions of the particles at 4 times within the simulated timespan are shown. The radius of the markers indicates the mass of the particles. This figure shows that the particles moved in the negative x- and y-direction and their mass is increasing. The rate of spreading of the particles is similar to the forward simulations.

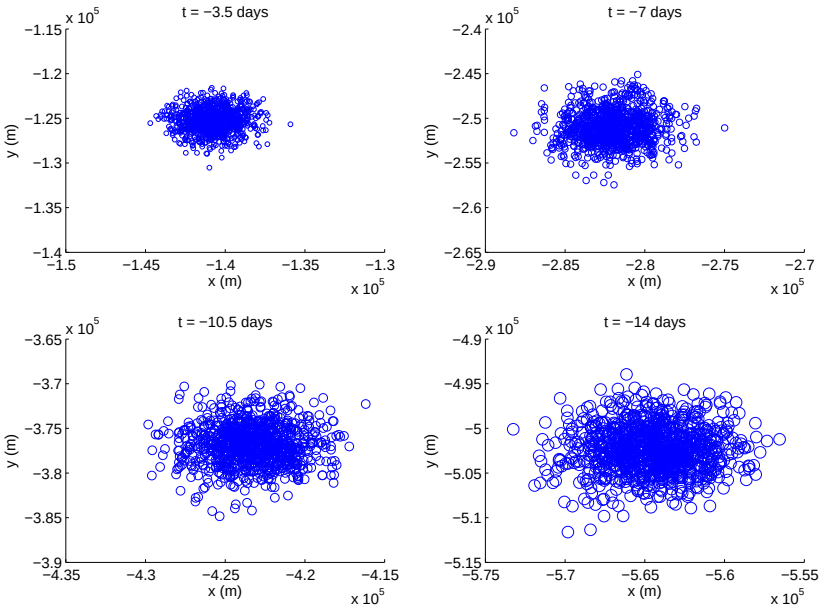

Figure 6.23: These figures show the macroplastics at 4 times for the reverse time simulations. The mass of the particles (indicated by the radius of the markers) is increasing over time. The particles are moving in the negative x- and y-direction and the spreading of the particles is increasing.

6.3.4. Reverse-time simulations for microplastics

For the microplastics similar figures are made of the reverse time simulations. These simulations were done with the improved settling rate that is inversely proportional to the water depth.

The first figure in this section is again a histogram. Similar to the histogram in the previous section, the bars are the sum of the 'weighted mass' of the particles in that bin. The shape of the histogram is also similar to the previous histograms. The highest bars are located in the centre of the area and lower bars are at the edges.

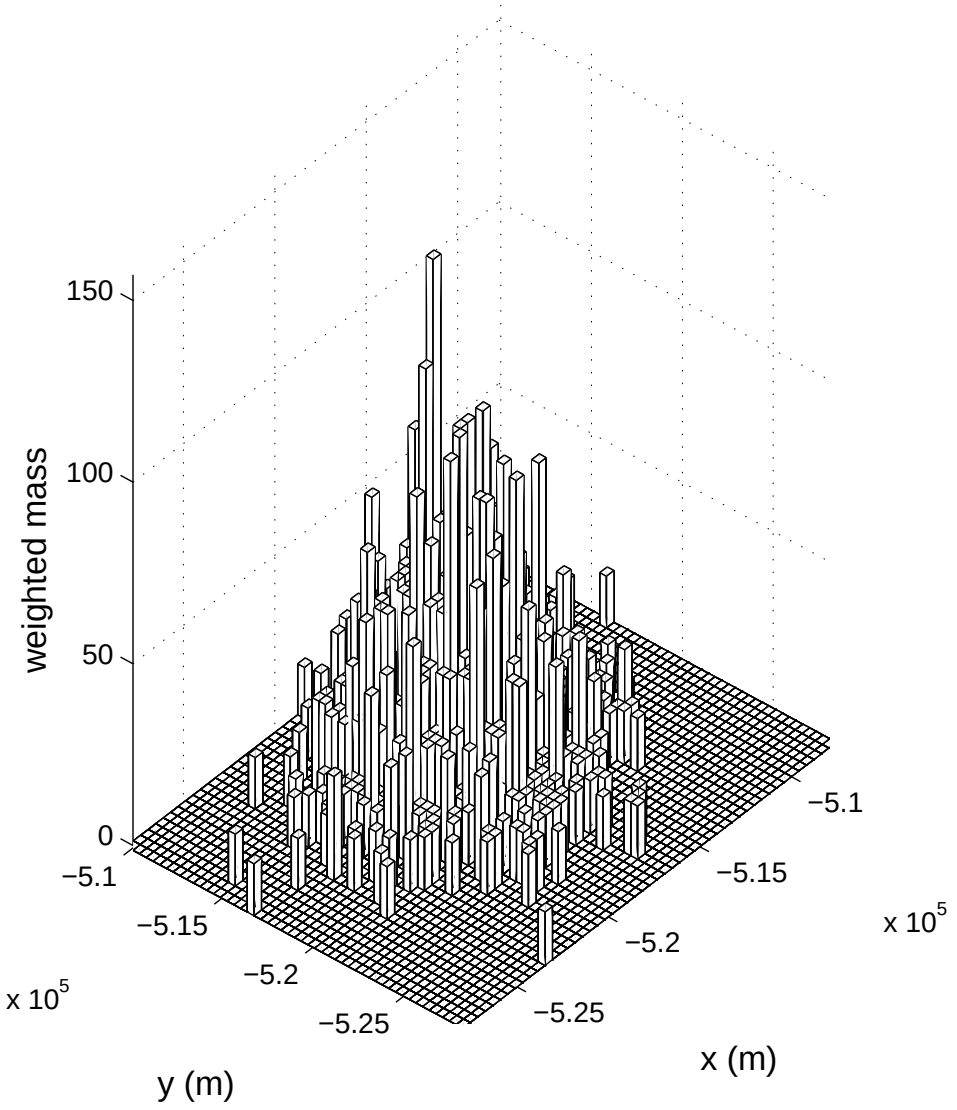

Figure 6.24: This figure is a histogram of the area where microplastics were positioned after the reverse time simulation. The height of a bars equals the sum of the mass multiplied by the weight of the particles in that bin. This means that a higher bar is equivalent to a higher probability that particle was originated at that position.

The next two figures show what path the microplastics followed in the reverse time simulations. The starting point was (0,0) and the particles moved in the negative x- and y-direction. In the first figure the light line indicates the path that would be used if there was no dispersion and the blue lines are the paths taken with dispersion. Like the previous simulations, the particles are spread out more as they move further from their source due to dispersion. In the second figure the increase in mass is visible. The colour of the graph indicates the mass at that point. The figure shows that the mass of the particles increased over time. As expected the position and mass of the microplastics is changing in the opposite direction compared to the forward simulations.

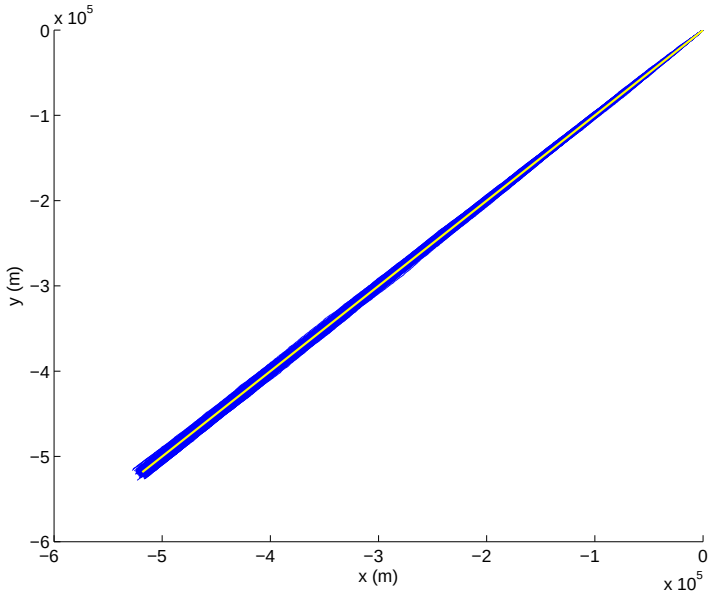

Figure 6.25: In this figure the reverse time paths of all the microplastics are plotted together. The starting point was (0,0) and the particles are moving in the negative x- and y-direction. The light line shows the path taken when there would be no dispersion. As the particles are moving further from their source the variation from the path without dispersion is increasing.

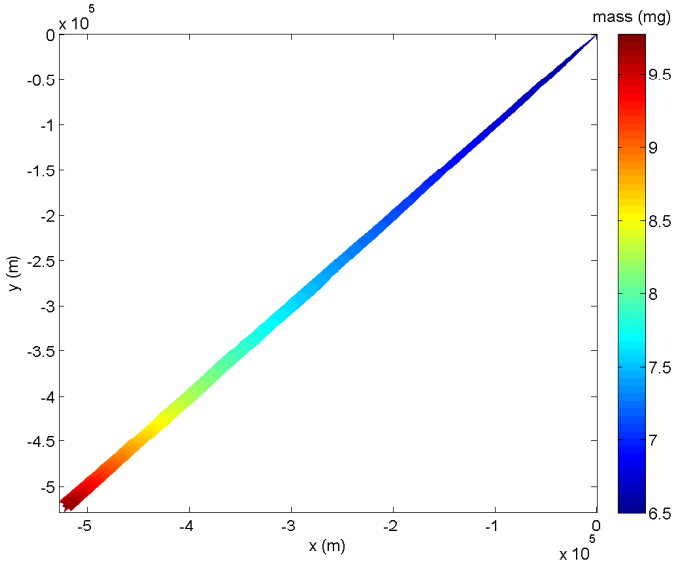

Figure 6.26: In this figure the reverse time paths and mass of all microplastics are plotted. The starting point was (0,0) and the particles are moving in the negative x- and y-direction. The mass of the microplastics was 6.5 mg at the starting point. The colour of the graph indicates the weight of the particles. The mass is increasing as the particles move further from their starting point because the process of settling is reversed in these simulations.

In the next figure the position of the microplastics at 4 times within the simulated timespan are shown. This figure also shows that the particles moved in the negative x and y direction and both their mass and spreading are increasing.

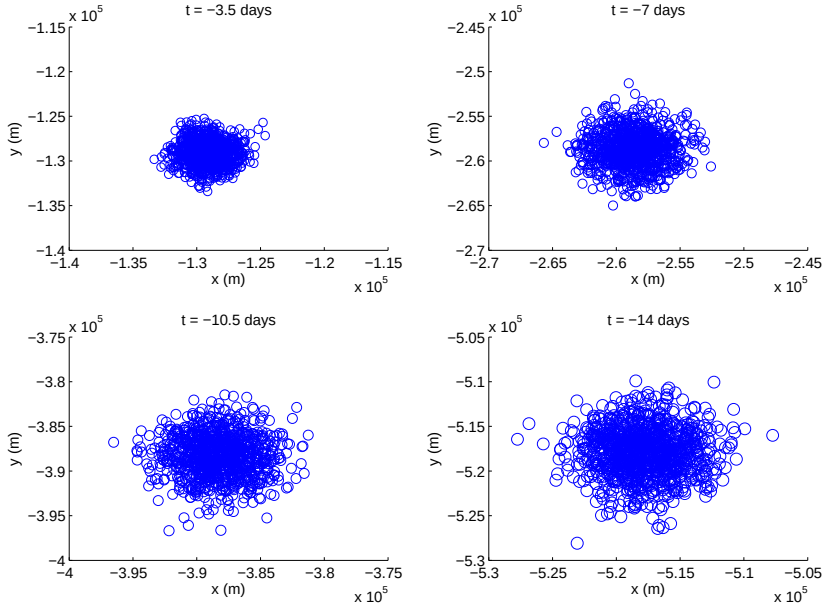

Figure 6.27: These figures show the microplastics at 4 times for the reverse time simulations. The mass of the particles (indicated by the radius of the markers) is increasing over time. The particles are moving in the negative x- and y-direction and the spreading of the particles is increasing.

7

Conclusions and recommendations

In this last chapter the final conclusions of this project will be drawn and some recommendations for further research and improving this model will be made.

7.1. Conclusions

This project had two main goals. The first goal was to add the settling of particles to the forward advection-diffusion equation. To achieve this, two different methods were used. Both led to the same result, an extra term in the advection-diffusion equations containing the settling rate γ. Using the Lagrangian random walk model, a numerical approximation for this advection-diffusion equation was found.

The simulations using this numerical solution were compared with simulations using the standard advection-diffusion equation and settling probabilities. For macroplastics the results of both simulations were right away similar. For microplastics the results were less successful at first. This could be explained by the fact that the settling probability for microplastics was depending on the water depth, while the settling rate was defined constant. The simulations were repeated with a settling rate inversely proportional to the water depth and these results were much more successful.

The second goal was to derive the reverse time advection-diffusion equation that included the settling. The reverse time advection-diffusion equation was derived by calculating the adjoint of the Kolmogorov forward equation and rewriting this into the form of an advection-diffusion equation. This same method was used on the settling term. The adjoint of the settling term was derived and added to the backward Kolmogorov equation. This could also be rewritten to a reverse time advection-diffusion equation that included terms for the settling of particles.

Again the Lagrangian random walk method was used to find a numerical approximation for the reverse time advection-diffusion equation. Compared to the numerical approximation of the forward equations, this resulted in an extra weighing function.

As expected the results for the reverse time simulations were quite similar to the forward time simulations. The direction of the particle movement was in the reverse time simulations was exactly opposite to the direction in the forward time simulations. The mass of the particles was increasing instead of decreasing over time. Due to the simplified situation that was modelled, the weighing function that was added for the reverse time models did not have a very distinctive effect on the results. It can be assumed that the weighing function would have a more important effect when the test case is less simple.

7.2. Recommendations

The simulations of this project were done for a general situation and therefore it is hard to test their accuracy. The results of this project could be validated by using empirical data of a specific location and doing simulations with parameters corresponding to this location. This way the simulations can be compared with actual data to check how accurate this model is and to see which improvements could be made.

The model could be improved by taking more of the oceanic properties into account. Quite some aspects are now simplified or not taken into account. This was already mentioned for some simplified parameters,

like current, diffusivity and water depth. However, other properties like salinity and water temperature could also be taken into account to make a more realistic model. A difficulty in including these properties in the model is that there is not much research available for most of these parameters. Moreover their characteristics are very site specific so the research that is done in some coastal areas can often not be applied to model other areas of interest.

In further research it could be tried to incorporate other processes in the advection-diffusion equation in a similar way as the settling of particles. For example processes like the degradation of macroplastics or particles landing on the beach could maybe be incorporated in the advection-diffusion equation using similar methods as those used in this report to include the settling of particles. Incorporating these processes in the advection-diffusion equation would make it easier to also do reverse time simulations of these processes.

Bibliography

[1] M. Brics, J. Kaupužs, and R. Mahnke1. How to solve fokker-planck equation treating mixed eigenvalue spectrum? *Condensed Matter Physics*, 16, 2013.

[2] Wilson Mahera Charles. *Transport modelling in coastal waters using stochastic differential equations*. PhD thesis, TU Delft, March 2007.

[3] K. Critchell, A.Grech, J.Schlaefer, F.P.Andutta, J.Lambrechts, E.Wolanski, and M.Hamann. Modelling the fate of marine debris along a complex shoreline: Lessons from the great barrier reef. *Estuarine, Coastal and Shelf Science*, 167:414 – 426, December 2015.

[4] Kay Critchell and Jonathan Lambrechts. Modelling accumulation of marine plastics in the coastal zone; what are dominant physical processes. *Estuarine, Coastal and Shelf Science*, 171:111 – 122, January 2016.

[5] Kay Critchell, Jonathan Lambrechts, and Eric Deleersnijder. Lagrangian modelling of plastic debris in coastal environment, July 2017.

[6] Britta Denise Hardesty and Chris Wilcox. Understanding the types, sources and at sea distribution of marine debris in australian waters, June 2011. URL `https://www.environment.gov.au/system/files/pages/8ff786ed-42cf-4a50-866e-13a4d231422b/files/marine-debris-sources.pdf`.

[7] Arnold Heemink. Numerical methods for stochastic differential equations. *Course notes*, August 2017.

[8] Janelle M. Hrycik, Joël Chassé, Barry R. Ruddick, and Christopher T. Taggart. Dispersal kernel estimation: A comparison of empirical and modelled particle dispersion in a coastal marine system. *Estuarine, Coastal and Shelf Science*, 133:11 – 22, November 2013.

[9] J.R. Hunter, P.D. Craig, and H.E. Phillips. On the use of random walk models with spatially variable diffusivity. *Journal of Computational Physic*, 106:366–376, 1993.

[10] Jenna R Jambeck, Roland Geyer, Chris Wilcox, Theodore R Siegler, Miriam Perryman, Anthony Andrady, Ramani Narayan, and Kara Lavender Law. Plastic waste inputs from land into ocean. *Science*, 347:768 – 771, February 2015.

[11] Nicole Kowalski, Aurelia M.Reichardt, and Joanna J.Waniek. Sinking rates of microplastics and potential implications of their alteration by physical, biological, and chemical factors. *Marine Pollution Bulletin*, 109:310 – 319, August 2016.

[12] MathWorks. pdepe: Solve initial-boundary value problems for parabolic-elliptic pdes in 1-d. (accessed at 11-08-2018). URL `https://nl.mathworks.com/help/matlab/ref/pdepe.html`.

[13] Akira Okubo. Oceanic diffusion diagrams. *Deep Sea Research and Oceanographic Abstracts*, 18:789 – 802, August 1971.

[14] S. Spagnol, E. Wolanski, E. Deleersnijder, R. Brinkman, F. McAllister, B. Cushman-Roisin, and E. Hanert. An error frequently made in the evaluation of advective transport in two-dimensional largangian models of advection-diffusion in coral reef waters. *Marine Ecology Progress Series*, 235:299 – 302, June 2002.

[15] Dar'ya Yakivna Spivakovs'ka. *Reverse-time diffusion in environmental models*. PhD thesis, TU Delft, September 2007.

[16] Hyder Ali Muttaqi Shah Syed. *Lagrangian modelling of transport processes in the ocean*. PhD thesis, TU Delft, September 2015.

[17] H.F.P. van den Boogaard, M.J.J. Hoogkamer, and A.W. Heemink. Parameter identification in particle models. *Stochastic Hydrology and Hydraulics*, 7:109 – 130, 1993.